AD-A238 390

AFIT/GST/ENS/91M-2

THE UTILITY OF ELLIPTICAL AND CIRCULAR CONFIDENCE REGIONS FOR HFDF RECEIVERS

THESIS

Paul T. Nemec, Captain, USAF

AFIT/GST/ENS/91M-2

DTIC
ELECTE
JUL 22 1991
S B D

Approved for public release; distribution unlimited

91-05763

91 7

REPORT DOCUMENTATION PAGE

Form Approved
OMB No. 0704-0188

1. AGENCY USE ONLY (Leave blank)	2. REPORT DATE	3. REPORT TYPE AND DATES COVERED
	March, 1991	Master's Thesis

4. TITLE AND SUBTITLE
The Utility of Elliptical and Circular Confidence Regions for HFDF Receivers

5. FUNDING NUMBERS

6. AUTHOR(S)
Paul T. Nemec, Captain, USAF

7. PERFORMING ORGANIZATION NAME(S) AND ADDRESS(ES)
Air Force Institute of Technology, WPAFB OH 45433-6583

8. PERFORMING ORGANIZATION REPORT NUMBER
AFIT/GST/ENS/91M-2

9. SPONSORING/MONITORING AGENCY NAME(S) AND ADDRESS(ES)
Department of Defense
Attn: R06
9800 Savage Road
Ft George G Meade MD 20755

10. SPONSORING/MONITORING AGENCY REPORT NUMBER

11. SUPPLEMENTARY NOTES

12a. DISTRIBUTION/AVAILABILITY STATEMENT
Approved for public release; distribution unlimited

12b. DISTRIBUTION CODE

13. ABSTRACT (Maximum 200 words)

This thesis investigates HFDF confidence region (CR) shape exhibited by geolocations in a search-and-rescue context. In Phase I, a Keeney-Raiffa multiattribute utility function was developed which allowed an analytical measure of preference between elliptical and equivalent-probability circular CRs. Phase II utilized a likelihood approach to establish CR shape for sample operational geolocations having multiple points of bearing intersections. For 12 sample Phase I geolocations, the elliptical CR always had higher utility than its corresponding circular CR. For accepted sample geolocations (circular CR area less than or equal to 3.142×10^4 n mi^2), a preference condition was developed whereby a circular CR would only be preferred over the corresponding elliptical CR if the relative percent utility difference was less than some DOD-established threshold percentage. Five out of the six rejected sample geolocations had elliptical CR eccentricities in excess of 0.98 suggesting the need for additional geolocation acceptability criteria. Further, one geolocation was falsely rejected as its elliptical CR area was less than the 3.142×10^4 n mi^2 value. In Phase II, near elliptically-shaped unimodal CRs were observed suggesting CR approximation by analytical means.

14. SUBJECT TERMS	15. NUMBER OF PAGES
Search and Rescue; HFDF Confidence Regions; Elliptical Confidence Region; Multiattribute Utility Function; Likelihood Function	87
	16. PRICE CODE

17. SECURITY CLASSIFICATION OF REPORT	18. SECURITY CLASSIFICATION OF THIS PAGE	19. SECURITY CLASSIFICATION OF ABSTRACT	20. LIMITATION OF ABSTRACT
Unclassified	Unclassified	Unclassified	UL

NSN 7540-01-280-5500

Standard Form 298 (Rev. 2-89)

AFIT/GST/ENS/91M-2

THE UTILITY OF ELLIPTICAL AND CIRCULAR CONFIDENCE REGIONS FOR HFDF RECEIVERS

THESIS

Presented to the Faculty of the School of Engineering
of the Air Force Institute of Technology
Air University
In Partial Fulfillment of the
Requirements for the Degree of
Master of Science (Operational Sciences)

Paul T. Nemec
Captain, USAF

March, 1991

Approved for public release; distribution unlimited

THESIS APPROVAL

STUDENT: CAPT PAUL NEMEC CLASS: GST-91M

THESIS TITLE: THE UTILITY OF ELLIPTICAL AND CIRCULAR CONFIDENCE REGIONS FOR HFDF RECEIVERS

DEFENSE DATE: 20 FEB 91

COMMITTEE:	NAME/DEPARTMENT	SIGNATURE
Advisor	Dr. James W. Chrissis, AFIT/ENS	
co-Advisor	Maj. Bruce W. Morlan, ENS	
Reader	Dr. Yupo Chan, ENS	

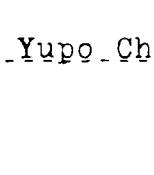

Accession For	
NTIS GRA&I	☑
DTIC TAB	☐
Unannounced	☐
Justification	
By	
Distribution/	
Availability Codes	
Dist	Avail and/or Special
A-1	

Acknowledgments

The completion of this thesis would not have been possible without the assistance of many people. First, a special thank-you is owed to my thesis advisor, Dr. James W. Chrissis. His timely insights and encouraging attitude helped me through the times when I doubted my ability to accomplish this task. I am also especially thankful for the efforts of Maj Bruce W. Morlan and Dr. Yupo Chan. Maj Morlan provided the impetus and technical depth I needed to perform the likelihood analysis in Phase II of this research and Dr. Chan provided expertise and perspective in the application of utility theory to confidence region preference. The assistance given by my thesis sponsors, Dr. Alfred Marsh and Capt David Drake was invaluable in formulating the utility function and was indeed deeply appreciated.

Finally, I would like to recognize most of all my wife, Susan, and my children, Ashley and Benjamin, for their loving support. Their devotion during this difficult period helped me to see how blessed a man I am.

Paul T. Nemec

Table of Contents

Acknowledgments ii

Abstract vi

I. Introduction 1

Background 1

Research Objectives 3

II. Literature Review 4

HF Propagation 4

Analytical Modeling of HFDF Bearing Errors 5

Fixing Algorithms and Ionospheric Prediction Models 9

Utility Functions 12

III. Phase I - Confidence Region Utility 17

Research Baseline 17

Study Procedure 17

Phase I Research 18

Model Formulation 25

Utility Function Development 25

Attribute Determination 25

Verification of Utility Independence . . 27

One-Dimensional Utilities and Scaling Factors 28
Formation of the Two-Dimensional Multiattribute Utility Function . . 30
Results 32
Confidence Region Parameters 32
Utility Function Formulation 33
Multiattribute Utility Calculations 36
Utility Comparisons 36

IV. A Likelihood Approach to Confidence Region Shape . 40
Research Baseline 40
Model Formulation 40
Results 43

V. Conclusions and Areas for Further Research 46
Conclusions 46
Areas for Further Research 49

Appendix A: Utility Function Input Data 51

Appendix B: Confidence Region Plots 57

Appendix C: Phase II FORTRAN and SAS Code 63

Appendix D: Likelihood Surfaces and Contours 67

Bibliography 77

Vita 79

Abstract

This thesis investigates HFDF confidence region (CR) shape exhibited by geolocations in a search-and-rescue context. In Phase I, a Keeney-Raiffa multiattribute utility function was developed which allowed an analytical measure of preference between elliptical and equivalent-probability circular CRs. Phase II utilized a likelihood approach to establish CR shape for sample operational geolocations having multiple points of bearing intersections.

For 12 sample Phase I geolocations, the elliptical CR always had higher utility than its corresponding circular CR. For accepted sample geolocations (circular CR area $\leq 3.142 \times 10^4$ n mi^2), a preference condition was developed whereby a circular CR would only be preferred over the corresponding elliptical CR if the relative percent utility difference was less than some DoD-established threshold percentage. Five out of the six rejected sample geolocations had elliptical CR eccentricities in excess of 0.98 suggesting the need for additional geolocation acceptability criteria. Further, one geolocation was falsely rejected as its elliptical CR area was less than the 3.142×10^4 n mi^2 value.

In Phase II, near elliptically-shaped unimodal CRs were observed for the operational geolocations studied. These results suggest operational CR approximation via analytically derived elliptical CRs.

The Utility of Elliptical and Circular Confidence Regions for HFDF Receivers

I. Introduction

Background The United States operates a worldwide network of receiving stations which perform a Search and Rescue (SAR) mission. These stations both receive and process distress signals from airplanes and ships at random points along documented traffic corridors. A minimum of three receiving stations are required to process a distress signal in order to produce a position estimate and then commence a SAR mission. Each station contains two complementing systems which perform the geolocation of the signal transmitter. The first, the Receiving Subsystem (RS), is primarily used to detect the emergency transmission and begin the geolocation process which the High Frequency Direction Finding subsystem (HFDF) completes resulting in an estimated location of the signal transmitter. All stations contain one RS and a range of from zero to ten HFDF resources. Further, each RS can sample the entire transmitter frequency range of interest while each HFDF resource can cover at most a single assigned 1 MHz band of this range (3:1-2).

In light of the frequency coverage limitations of the HFDF subsystems, the optimal allocation of frequencies that increases the probability of successful geolocation must be determined. To accomplish this optimization, each station's line-of-bearing to the transmitter area must result in a geolocation with an acceptable elliptical confidence region. The confidence region is elliptical due to the underlying bivariate-normal distribution chosen for the fix estimates. This region establishes the area of transmitter location to a Department of Defense (DOD) selected probability of 0.9 (3:2,4,7-9).

The DOD has established an objective function to maximize the expected number of geolocations in a SAR network. By approximating the confidence ellipse with a circle of equivalent area, the radius can be used as an acceptability criterion for candidate HFDF station combinations. A maximum allowable confidence region radius is incorporated into the objective function by way of an indicator function. This indicator function is either assigned a value of one (highest utility) if the equivalent circle radius of the confidence region is less than some acceptable nautical mile limit, or a value of zero (lowest utility) otherwise (3:9).

Recent work in this area of the SAR mission has focused on obtaining an optimal frequency assignment to known HFDF

systems using a multiobjective linear programming technique. However, this work did not explicitly address the confidence region radius limitation (11:vii). Analysis of the possible elliptical and circular confidence regions for any geolocation can aid decision makers in determining the most promising geolocations for the allocation of SAR resources.

Research Objectives In order to supplement the results of current work in this area, emphasis is placed on the examination of circular and elliptical confidence regions to understand how attributes such as shape and area could impact SAR operations. The purpose of this research is twofold. First, Phase I establishes an analytical measure of preference between an elliptical confidence region and its corresponding equivalent-probability circular confidence region. A utility function establishes this preference measure. As used in this objective statement, utility is defined as the value that a decision maker would attach to a number of competing alternatives (13:25). Second, Phase II examines the confidence region shape exhibited by operational geolocations with the aim of developing a measure of validity for the analytical results of Phase I.

II. Literature Review

The discussion which follows highlights literature relevant to accomplishing the objectives of this research The review addresses topics in the following areas: 1) the concepts behind high frequency (HF) propagation; 2) the presence, nature, and modeling of errors in high frequency direction finding (HFDF); 3) the various algorithms in use for fixing the location of HF transmissions; and 4) the theory and development of utility functions.

HF Propagation In a Search and Rescue (SAR) context, HF radio is the primary means of establishing communication between the shore and seagoing vessels in distress. HF can propagate either by means of a groundwave or through the atmosphere as a skywave. Because groundwave propagation is limited to a practical maximum distance of 300 miles over sea, propagation by skywave is more likely for SAR missions. Skywave propagation is due to the refracting or bending of the HF energy wave by the ionosphere. It is the skywave that allows HF communications of up to 4000 miles in a single refraction or hop (9:1-8).

Several ionospheric phenomena affect skywave propagation. Jannusch categorizes these phenomena as follows: 1) the layered nature of the ionosphere; 2) solar induced changes; 3) daily, seasonal, and geographic variations; and 4) changes induced by the earth's magnetic

field. Of the four identified layers of the ionosphere, the outermost or F region is the most efficient for skywave propagation. This region is found at altitudes ranging from 100 to 200 miles. In conjunction with the other layers, however, multi-mode propagation effects can occur when the HF wave refracts at more than one layer, resulting in multiple wave return paths for the same incident wave. The other phenomena listed above generally change the make-up of these layers. The following changes affect HF wave propagation: 1) electron density with time of day; 2) layer altitude with time of year; and 3) electron distribution with sunspot activity. Also, the presence of both travelling ionospheric disturbances and tilts changes the apparent height and location of refraction, thereby affecting the azimuthal or elevational angle of the return wave (10:14-18; 3:14). As defined by Heaps, tilts are "planes of constant electron density (that) are not precisely parallel to the earth" (8:11).

Analytical Modeling of HFDF Bearing Errors Bearing error is defined by Jannusch as "the difference between the azimuth angle from true north reported by a radio direction finding station and the true azimuth angle of the great-circle path to the transmitter" (10:8-9). Five types of bearing error are known to exist: 1) instrumental; 2) site; 3) wave-interference; 4) propagation; and 5) subjective. The first

three categories of bearing error can be reduced by the application of careful system design, by locating sites in places that minimize re-radiation of the arriving wavefronts and by the identification of multiple interfering rays. The last two bearing error types are not easily reduced. Propagation errors, which are produced by tilts in the ionosphere, are manifested by ray paths which deviate from the great-circle path containing the transmitter. Subjective errors are those errors caused by the human element interfacing with the system and can never be eliminated (10:8-10).

According to Heaps, propagation errors contribute the greatest to errors in position location (8:14). In a second article by Heaps, the ionospheric tilts and travelling ionospheric disturbances are responsible for the majority of the errors by introducing uncertainty in both the angle of the arriving wavefront and the altitude of the ionospheric refracting layer (7:8). The remainder of this review focusses upon these propagation errors.

Since errors associated with tilts and travelling ionospheric disturbances are not predictable, the measured line of bearing must be modeled as a random variable with some form of probability distribution. The simplest model used to describe a population of bearing errors is based on the assumptions that individual bearing errors are

independent of each other and that they have a normal distribution with constant mean and variance. The most widely used form of this model has a mean equal to zero and a variance which is a function of various environmental factors such as the time of day. Models which rely on environmental factors use some type of variance predictor in order to arrive at a reasonable expected value for use in fixing algorithms. A second category of models is known as leptokurtic models because they generate a population distribution with a larger measure of peakedness (kurtosis) than that of the normal distribution. This type of distribution is built by overlaying a normal distribution upon a uniform distribution. As in the simple model developed above, the propagation errors are largely normal while the uniform distribution describes the probability that a particular bearing is a wild bearing. A wild bearing can be any bearing which is outside an established true error limit. Ten degrees is a common limit used (4:24-32).

Given the bearing errors modeled by the above mean, the development of a confidence region is necessary to establish a degree of location certainty. Felix defines a confidence region as "a region which will include the true target position some given percentage of the time, based on the distribution of error" (4:71). Since each fix estimate will possess its own confidence region, the confidence region of

a number of identically taken fixes is calculated as the ratio of successful overlaps of the true target position to the total number of fixes (4:71).

The confidence region is also related to the distribution selected for the fixes. Since range and azimuth variables are necessary to establish a fix estimate, a bivariate-normal distribution can be used with the assumptions developed previously for the univariate case. For multiple fixes, the confidence region would appear somewhat elliptical, centered about a mean range and azimuth point. The major and minor axes defining the ellipse would be in the range and azimuth directions (14:1-2).

Mathematical relationships have been developed to define these elliptical confidence regions. For a 90% confidence ellipse, Reilly defines the region as

$$\frac{x^2}{\sigma_x^2} + \frac{y^2}{\sigma_y^2} = 4.605$$

where X and Y are the fix coordinates in the XY plane, and σ_x and σ_y are the standard deviations for the sample of fixes in the X and Y directions respectively (14:2-5). Analytical relationships have also been developed by the Department of Defense (DOD) for computing the parameters defining HFDF confidence ellipses. The results can be used to calculate major axis orientation, lengths of both the

major and minor axes, and the area of the ellipse. The final results are summarized in Figure 1. The constants A′, B′, and C′ are functions of the bearing β_i from the transmitter to station i, the standard deviation σ_i of the bearing from station i, and the angle ψ_i subtended at the earth's center by the great circle range to the transmitter from station i. The radius of the earth is denoted by ρ. The DOD made several assumptions in its derivations: 1) line of bearing projections are straight lines; 2) an observation error displaces a line of bearing parallel to itself; 3) the true range is significantly greater than the error in its estimate; and 4) the earth is flat in the area of interest (2: all).

Fixing Algorithms and Ionospheric Prediction Models Unlike the analytical algorithms discussed above, fixing algorithms are used operationally to arrive at position estimates. Fixing algorithms can be categorized by the approach each one takes to determine a best-point-estimate of location from a sample of bearings. Three types of approaches exist: 1) geometric; 2) multiple regression; and 3) non linear programming.

FFIX is an algorithm which uses a geometric approach. It features a maximum likelihood method which locates a

Orientation of the major axis:

$$\phi'_{max} = \frac{1}{2}\tan^{-1}\left(\frac{2C'}{A'-B'}\right) + \frac{\Delta'\pi}{2} \quad , \quad -\pi/2 \leq \tan^{-1}\frac{2C'}{A'-B'} < \pi/2 \tag{34a}$$

$$\Delta' = \begin{cases} 0, & A'-B' \geq 0 \\ 1, & A'-B' < 0 \end{cases} \tag{34b}$$

One half the length of the major axis:

$$r_{max} = \left[\frac{-2\rho^2 \ln(1-P)}{A'\sin^2\phi'_{max} - 2C'\sin\phi'_{max}\cos\phi'_{max} + B'\cos^2\phi'_{max}}\right]^{1/2} \tag{35}$$

One half the length of the minor axis:

$$r_{min} = \left[\frac{-2\rho^2 \ln(1-P)}{A'\cos^2\phi'_{max} + 2C'\cos\phi'_{max}\sin\phi'_{max} + B'\sin^2\phi'_{max}}\right]^{1/2} \tag{36}$$

Area of the ellipse:

$$A_e = \frac{-2\pi\rho^2 \ln(1-P)}{\sqrt{A'B'-C'^2}} \tag{37}$$

$$A' = \sum_{i=1}^{n} \frac{\cos^2\beta_i}{\sigma_i^2 \sin^2\psi_i} \quad , \quad B' = \sum_{i=1}^{n} \frac{\sin^2\beta_i}{\sigma_i^2 \sin^2\psi_i} \quad , \quad C' = \sum_{i=1}^{n} \frac{\sin\beta_i \cos\beta_i}{\sigma_i^2 \sin^2\psi_i} \tag{38}$$

ϕ'_{max} measured CW from north

β_i bearing from target to i^{th} DF site, CW from north

Figure 1. Elliptical Confidence Region Parameters (2: 21)

position estimate by finding a point whose squared distance from all other points is a minimum. Other information provided by this algorithm includes confidence ellipse parameters and a chi square statistic which represents the goodness of fit of the sample error distribution with a true normal distribution. This statistic is also used to identify wild bearings (4:44-49).

The second type of algorithmic approach is used by NOSCLOC. This model provides a minimum value for both the unbiased variance estimate of position and the confidence region area (4:50-55).

The nonlinear programming approach is used by FALCONFIX. Unlike the previous algorithms, which eliminate wild bearings, FALCONFIX uses all bearings to determine a most likely position. The algorithm uses a bearing variance model which uses an error distribution referred to as a composite normal-uniform which is similar to those of the leptokurtic models discussed earlier. The standard deviation of the bearing errors is used to arrive at a likelihood function. Each possible mode or maxima of this function is determined using gradient search techniques. These techniques attempt to find the direction of movement along a surface which will lead to the greatest increase in the likelihood function. The resulting points represent position estimates (4:58-61).

Accuracy obtained using these fixing algorithms can be enhanced by the use of ionospheric prediction models. Rather than just statistically rejecting wild bearings as is done in the FFIX and NOSCLOC algorithms, models such as the Tactical Prediction Model (TPM) can be used to assist in the bearing selection process. TPM can provide usable frequency ranges over specific paths, skywave propagation probability for the paths, and plots of bearing variance as a function of propagation factors. Bearing selection can also be enhanced by the use of doppler difference frequency techniques which permit the detection of travelling ionospheric disturbances and multimode propagation. From the results of Jannusch's work, it was clear that both the use of TPM and travelling ionospheric detection techniques improved fix estimation (10:19-23,63).

Utility Functions A utility function can be described as a means of representing nonlinear preferences for possible benefits and losses in situations that involve uncertainty. The concept of utility measurement permits the creation of such utility functions. The axiomatic basis for the utility function leads to two practical results: 1) the utility of a consequence can be measured on an ordered metric scale permitting subsequent calculations and analysis; and 2) the measurement of utility is an equivalency procedure using probabilities as weights (1:352-371).

Two primary methods exist for measuring one-dimensional utility. The first is a certainty equivalent or fractile method. This approach establishes points on the utility curve by establishing the outcomes which are valued equally to some binary stimulus lottery whose outcomes are set initially at the extremes of the range. This method uses the same probability in all stimulus lotteries. In general, a lottery can be defined as a set of possible outcomes, X_i, with probability of occurrence P_i which can be written (X1,P1; X2,P2; ...). A binary lottery contains only two outcomes with complementary probabilities and can be represented by (X1,P1; X2).

The second method of measuring utility is referred to as the lottery equivalent/probability. As the name implies, a binary lottery is made equivalent to a binary stimulus lottery whose outcomes are fixed at the extremes of the range. By varying the probability equivalent, P_e, outcomes are generated whose utility can be shown to always equal $2P_e$.

In calculating the above utilities, both methods use an important result of the utility axioms:

$$U(\text{lottery}) = \sum P_i \times U(X_i)$$

Once discrete points representing the utilities of various outcomes have been measured, an analytic function can then be fit. Two kinds of functional forms presently in use include the exponential, $U(X) = a + be^{-cx}$, and the power function, $U(X) = a + bX^c$, where a, b, and c represent characteristic parameters (1: 373-384).

Since many situations exist requiring analysis of consequences with more than one dimension, analytic methods for measuring preferences of such consequences have been developed. Keeney-Raiffa multiattribute utility is one approach which is preferred to other more elementary models. Two assumptions on the structure of preferences provide the basis for the theory. The first, preferential independence, states that the ranking of preferences over any pair of attributes given some level of the other attributes will be maintained for all levels of these other attributes. The second assumption is utility independence. This assumption provides that the indifference between a lottery and a certainty equivalent for any attribute given some level of a different attribute, is not affected by the levels of these different attributes. With these two assumptions, the Keeney-Raiffa multiattribute utility function $U(X)$ is defined

$$KU(\boldsymbol{X}) + 1 = \prod (Kk_i U(X_i) + 1) \qquad (1)$$

where $U(X_i)$ are one-dimensional utility functions, K is a normalizing factor which maintains consistency between the defined scaling of the Keeney-Raiffa multiattribute utility function $U(\boldsymbol{X})$ and the $U(X_i)$, and k_i is a scaling factor for each attribute dimension. Each k_i represents a multiattribute utility when attribute i is at its most desirable level and all other attributes at their least desirable levels: $(X_i^*, X_{j\bullet}) \sim (\boldsymbol{X}, P_i; \boldsymbol{X})$. In the two-dimensional case, an explicit solution for $U(\boldsymbol{X})$ exists:

$$U(X_1, X_2) = k_1 U(X_1) + k_2 U(X_2) + (1-k_1-k_2)U(X_1)U(X_2) \qquad (2)$$

where k_i can be shown to equal P_i (1: 396-419).

In summary, this literature review provided information essential to accomplishing the objective of this research. The review began with a look at HF propagation. The skywave propagation of HF radio waves is subject to various ionospheric phenomena. Some of the more significant effects include the presence of travelling ionospheric disturbances and tilts. These effects produce the majority of propagation errors which result in HFDF bearing errors.

These bearing errors are most commonly modeled as random variables having a normal distribution. When distributed in this manner, confidence regions are elliptical in shape and have been mathematically defined. Using this background, common fixing algorithms in use today were reviewed. With the proper application of ionospheric prediction techniques, these fixing algorithms can provide better fix estimation. Finally, on a topic somewhat separate from the prior material, utility functions were discussed with emphasis on utility measurement and the concepts of multiattribute utility.

III. Phase I - Confidence Region Utility

This chapter presents the methodology used in executing Phase I of this research and the results obtained. Particular areas of the methodology addressed include a set of conditions for the research, a step-by-step study procedure, and a discussion of model formulation. Chapter IV provides a similar development for Phase II of this research.

Research Baseline The following conditions establish a baseline from which this research proceeds.

1. As was in evidence during the literature review, many fixing algorithms exist to estimate a transmitter location. In order to consistently compare the results of this research, the confidence area mathematics developed by the DOD was used.

2. This research was not concerned with obtaining an optimal frequency allocation to the known HFDF systems. Particular receiver station characteristics, such as the established number of HFDF assets per station and the specific frequency assigned to each asset, were therefore not considered factors.

Study Procedure The procedure discussed below permitted the determination of preference for elliptically shaped confidence regions over equivalent-probability circular regions. The steps included were as follows: 1) gathering

data for the geographic region being studied; 2) calculating the necessary ellipse and equivalent circle parameters for randomly generated geolocations; 3) calculating confidence region utilities; and 4) determining confidence region preferences.

Phase I Research. Work on the Phase I effort began with data gathering using existing data provided by the DOD. The following data was necessary: 1) latitude and longitude of both the appropriate HFDF receiving stations and transmitting location; 2) the standard deviation of the bearings from each receiving station; and 3) an acceptable circular confidence region radius value (d_i) for the transmitting location.

Using established locations of SAR transmitter areas, the North Sea area was arbitrarily selected for this research. The location of this transmitter area, in decimal degrees, is 57.33N and 2.03E. Its acceptable circular confidence region radius is 100 nautical miles. The subset of candidate receiver stations were selected from a total of 30 worldwide sites. The necessary data for those sites is included in Table 1. All sites except the one in San Francisco, CA were chosen because of their close proximity to the North Sea area (12: all).

TABLE 1

CANDIDATE HFDF RECEIVER STATIONS

HFDF Receiver Site	Location (decimal deg)		Bearing σ (rad)
San Francisco, CA (R01)	37.75N	122.43W	.1208359
Ribeira Grande, Azores (R07)	37.78N	025.50W	.0622357
Norfolk, VA (R08)	36.88N	076.27W	.0902294
Bangor, ME (R09)	44.75N	068.83W	.0759217
St. Johns, Newfoundland (R10)	47.55N	052.67W	.0604329
Reykjavik, Iceland (R14)	64.15N	021.95W	.0473332
Montrose, Scotland (R15)	56.75N	002.75W	.0841106
Cadiz, Spain (R16)	36.53N	006.30W	.0421765
Munich, W. Germany (R17)	48.07N	011.70E	.0432817
Brindisi, Italy (R18)	40.63N	017.93E	.0392714
London, England (R20)	51.83N	000.00W	.0654783
Athens, Greece (R21)	37.98N	023.73E	.0573793
Paris, France (R22)	48.87N	002.47E	.0518221
Stockholm, Sweden (R29)	59.33N	018.08E	.0511218

Once the necessary data was obtained, random geolocations were established consisting of three HFDF receivers each. The procedure following was used to establish a sample of ten random geolocations.

1. The first nine geolocations were established from the sample of sites listed in Table 1 less the site at San Francisco, CA. The tenth geolocation was

established from the 30 HFDF sites available worldwide and was included to recognize the possibility of obtaining a geolocation with a bearing from a remote sensor site. It was the tenth geolocation which included the San Francisco site.

2. Random numbers in sets of three were generated across a range equal to the number of available sites. The numbers were then rounded to the nearest integer.

3. After ordering the sites used for the first nine samples as shown in Table 1, the geolocations were generated by matching the random integer value to the receiver site with that same position in the order. The tenth geolocation was established similarly with the 30 sites ordered as shown in the previously referenced DOD letter.

Two additional geolocations were selected so as to include bearings from the closest sensor sites (geolocation #11) in combination with smaller bearing standard deviations (geolocation #12). The 12 resulting geolocations are presented in Table 2.

For each of the 12 geolocations both the elliptical and circular confidence region parameters were calculated as discussed below. Using equations from the DOD Technical Memorandum (2: 25), functions of the angles ψ and β were first determined. ψ represents the angle subtended at the

TABLE 2

SAMPLE GEOLOCATIONS

Geolocation #	HFDF Stations
1	(R09,R14,R21)
2	(R08,R14,R20)
3	(R08,R09,R29)
4	(R07,R16,R17)
5	(R08,R09,R15)
6	(R16,R20,R22)
7	(R20,R21,R29)
8	(R10,R17,R21)
9	(R07,R15,R18)
10	(R01,R07,R18)
11	(R14,R15,R29)
12	(R14,R17,R29)

earth's center by the great circle range from the receiving station to the transmitting location. β represents the bearing from the transmitter to the receiving station measured clockwise from North. These angles were then used to calculate the intermediate values A', B', and C' followed by the ellipse parameters Ae (ellipse area), rmin (one-half of the minor axis length), rmax (one-half of the major axis length), and ϕ'max (major axis orientation) as defined in Figure 1. All of these computations were accomplished using the MathCad software. For the equivalent-probability

circular region, the following approach was used for parameter calculation, as developed by Harter (6:all).

1. It was assumed that the two variables x and y, which represent the orthogonal components of the transmitter miss distance, were normally and independently distributed. Further, the components each had zero mean and standard deviations of σ_x and σ_y, labelled such that $\sigma_x \geq \sigma_y$.

2. The standard deviations were calculated using equations developed in the DOD Technical Memorandum:

$$\sigma_\varepsilon = \sqrt{\frac{b}{ab-c^2}}$$

$$\sigma_\eta = \sqrt{\frac{a}{ab-c^2}}$$

where $a = \frac{1}{\rho^2} \times A'$, $b = \frac{1}{\rho^2} \times B'$, $c = \frac{-1}{\rho^2} \times C'$, and ρ is the radius of the earth in statute miles. The values A′, B′, and C′ are the same intermediate values calculated above.

3. After re-labelling the above values σ_x and σ_y such that $\sigma_x \geq \sigma_y$, the value $c = \frac{\sigma_x}{\sigma_y}$ was calculated. This value should not be confused with the variable c defined in

the DOD Memorandum.

4. Using this calculated c value and letting the cumulative probability P equal 0.90 as for the elliptical confidence region, Table 2 from Harter (6:728) was used to determine the K value. The K value represents a multiplier used in calculating the radius of the equal-probability circle. Linear interpolation was used when necessary in determining the K values.

5. Finally, the radius of the circular region containing 90% of the transmitter position estimates was found by calculating $K\sigma_x$.

The discussion that follows illustrates the approach taken in determining confidence region preferences. The approach examines preferences for instances where geolocations would be both accepted and rejected under current practice. Preferences between the elliptical and circular confidence regions were determined from the above parameters using a developed utility function. The specifics of the utility function development and calibration are included in the section on model formulation.

Geolocations are currently accepted if the circular confidence region area is less than some established critical value. For those geolocations currently accepted, confidence region preferences were ultimately based on the

magnitude of the difference between the utilities of both the elliptical and circular regions. Since the elliptical confidence region will always have higher utility (see utility function formulation), the circular confidence region will only be preferred when the following condition holds:

$$\frac{U(\text{elliptical CR}) - U(\text{circular CR})}{U(\text{elliptical CR})} \times 100 \leq \delta \qquad (3)$$

where δ is a threshold percentage to be established by the DOD. The above calculation provides a measure of the percent of utility lost through the use of the circular confidence region. δ represents the minimum loss percentage necessary to justify use of the elliptical confidence region.

In the instance where geolocations are currently rejected (i.e. the circular confidence region area is greater than some established value), confidence region preferences will be determined based on the area of the corresponding elliptical region. If the area of the elliptical region is less than the critical value, it will be preferred. Utility evaluations in this case carry added significance in that they will determine if a "good" geolocation was in fact rejected. If the elliptical region area is also greater than the critical area, neither region

will be preferred.

Model Formulation Model formulation for Phase I consisted of the development/calibration of a utility function to measure preferences among confidence region representations.

Utility Function Development. A multiattribute utility function of the Keeney-Raiffa form was chosen as the analytic method to measure confidence region preferences. Several steps were involved in developing such a function: 1) determination of the attributes or dimensions existing in the problem; 2) verification of the utility independence assumption; 3) measurement of the individual attribute utilities and scaling factors; and 4) determination of the multiattribute utility function of the form given by Eq (2). Each of these steps are discussed in detail.

Attribute Determination. In order to establish the most important attributes for this problem, a look back to the research objective may be useful. If the ultimate aim is to somehow aid the search and rescue (SAR) process, attention must be focussed on those confidence region parameters which affect the conduct of the SAR mission.

The most obvious parameter is the area of the confidence region. As the confidence region area decreases, the SAR mission has a greater chance of success and vice versa.

A second and somewhat less apparent parameter is that

of confidence region eccentricity, which is a measure of the degree of elliptical shape. Eccentricity is defined for an ellipse by the ratio $\frac{c}{a}$ where c is one-half the distance between the foci and a is one-half the major axis length. For any given acceptable confidence region area, the shape requiring the shortest search path distance to completely cover the confidence region would likely contribute more to SAR mission success. Since confidence region area and eccentricity are seen as two of the most influential attributes in measuring the differences between circular and elliptical confidence region approximations, only these two attributes are used in this research.

Having established the attributes, their appropriate ranges of values were determined. Also, from the extremes of these ranges, highest and lowest levels of preference were assigned. For the area attribute, expected values ranged from a minimum of near zero, which corresponded to a point location, to a maximum of 3.142×10^4 n mi^2, where the maximum allowable error radius is 100 nautical miles. The minimum range value is the most desired value of the area attribute while the maximum value is the least desired. The use of a circular area to define the least preferred confidence region area can be explained by the fact that the equivalent-probability circular region approximation will

always have greater area than the elliptical region it approximates. Therefore, the maximum allowable area will always correspond to that of the circular region.

For the eccentricity attribute, the range of values is, by definition, from a minimum of zero, which represents a circular shape, to a maximum of 1.0 which equates to a straight line. An eccentricity of one is most desirable while a value of zero is least desirable. This can best be seen by using a search example. For eccentricities close to one, the resulting search area could conceivably be completely covered by a single search path. As eccentricities approach zero, multiple search paths may be required to cover the entire area which will therefore require a longer total search path.

Verification of Utility Independence. As was discussed in Chapter 2, both preferential and utility independence assumptions form the basis of multiattribute utility theory. For the two-dimensional case, however, only the concept of utility independence has relevance since preferential independence looks at the order of ranking existing between pairs of attributes for given levels of other attributes. Utility independence must be verified for area relative to eccentricity, and vice versa.

The utility independence of area is established when, for all levels of eccentricity, an indifference statement

between several levels of area remains valid. Using the following indifference result provided by the DOD as an example, utility independence for area would exist if the probability value of 0.25 remained constant for all given values of eccentricity:

$$(0, P=0.25; 3.142\times10^4) \sim (0.5(3.142\times10^4), 0.50; 3.142\times10^4)$$

For eccentricity values near the bounds of the range, say 0.1 which corresponds to a highly circular region and 0.9 which represents a very narrow elliptical region, it is reasonable to believe that the indifference probability will remain near 0.25 in either case. The decisionmaker, irrespective of confidence region eccentricity, will continue to favor the first lottery for values of $P > 0.25$ since this represents the probability of getting a confidence region area of near zero. The eccentricity of such a region is of course meaningless. When viewed in terms of the chance of getting the maximum area region, the first lottery will also be favored only for lower values of (1-P), say 0.6 to 0.7, since these regions are equally unattractive with higher values of (1-P) regardless of their shape. In a similar manner, the utility independence of eccentricity relative to area could also be argued.

One-Dimensional Utilities and Scaling Factors. Measurements were made to allow formulation of utility

functions and scaling factors for both the area and eccentricity attributes. The lottery equivalent/probability (LEP) method was employed to obtain the necessary information.

For the eccentricity attribute, the general LEP formulation is:

$$(1, P; 0.0) \sim (X_e, 0.50; 0.0)$$

where P represents an indifference probability and X_e a variable level of eccentricity. To find P, a series of questions were asked of the client/user utilizing a bracketing approach to close in on P. For a value of X_e=0.7 the series of questions had the form:

> If given the choice between either a 50:50 chance of getting an eccentricity, e, of 0.7 or 0.0 or a P:(1-P) chance of getting an eccentricity of 1 or 0, which would you prefer if P = 40%? 10%? 30%? or finally, 20%?

The user sequentially answered these questions until a P value was reached where he was indifferent between the two binary lotteries. Similar sets of questions were asked for various values of X_e with the result being (X_e, P) pairs from which utility values were calculated using the relation $U(X_e)=2P$. These values subsequently defined the utility function.

The same approach was taken for the area attribute.

Functional forms were then fit to these measurements thereby simplifying subsequent utility calculations. The characteristic parameters of the appropriate functional form resulted from the application of nonlinear regression analysis in the Statgraphics software.

A similar technique determined the scaling factors for each attribute. Again using eccentricity as an example, the LEP formulation has the general form:

$$(e \approx 1,\ A = 3.142 \times 10^4) \sim [(e \approx 1,\ A \approx 0),\ P\ ;\ (e = 0,\ A = 3.142 \times 10^4)]$$

where P again represents an indifference probability. A single set of questions like the ones above were used to obtain P. This value of P is the scaling factor. The complete questionnaire provided to the DOD and the four sets of responses obtained are presented as Appendix A.

Formation of the Two-Dimensional Multiattribute Utility Function. Having arrived at scaling factors and one-dimensional utility functions for both the area and eccentricity attributes, these quantities were then substituted into Eq (2). To better understand the genesis of this two-dimensional function, the following derivation is offered.

The multiattribute utility function is defined as follows:

$$KU(\boldsymbol{X}) + 1 = \prod (Kk_i U(X_i) + 1) \qquad (1)$$

where $U(\boldsymbol{X})$ is scaled from $U(\boldsymbol{X}_*)=0$ to $U(\boldsymbol{X}^*)=1.0$ and $U(X_i)$ is scaled from $U(X_{i_*})=0$ to $U(X_i^*)=1.0$ for the best and worst levels of X_i. An expression for the normalizing parameter K is now found by applying the above definitions for $U(\boldsymbol{X})$ and $U(X_i)$. Substituting $U(\boldsymbol{X})=1.0$ and $U(X_i)=1.0$ into Eq (1) gives the following result:

$$K + 1 = \prod (Kk_i + 1)$$

For the two-dimensional case, an explicit solution exists for K:

$$K = \frac{(1-k_1-k_2)}{(k_1 k_2)}$$

By substituting this into the expanded two-dimensional form of Eq (1), the final form of the utility function is obtained:

$$U(X_1,X_2) = k_1 U(X_1) + k_2 U(X_2) + (1-k_1-k_2)U(X_1)U(X_2) \qquad (2)$$

Results. This section displays the results obtained from Phase I. The presentation is in the following order: 1) elliptical confidence region parameters; 2) the equivalent

probability circular confidence region parameters; and 3) the utility results for both of the above regions.

Confidence Region Parameters. Table 3 captures the important 90% elliptical confidence region parameters for the 12 geolocations. Similarly, Table 4 lists the 90% circular confidence region parameters. As discussed in the methodology, the area of the circular confidence region was calculated using a radius of $K\sigma_x$.

In order to more easily visualize the area differences between the two confidence regions, plots containing traces of both regions were constructed for the 12 geolocations. These plots are presented in Appendix B.

TABLE 3

ELLIPTICAL CONFIDENCE REGION PARAMETERS

Geo. #	r_{max} (n mi)	r_{min} (n mi)	$A \cdot 10^4$n mi^2	ϕ'_{max} (rad)
1	871.026	72.510	19.736	2.274
2	94.627	46.081	1.370	0.049
3	559.566	56.627	9.947	1.235
4	120.459	57.462	2.175	-0.479
5	743.036	27.695	6.462	1.39
6	259.287	35.372	2.882	0.136
7	72.031	41.754	0.945	0.581
8	335.718	56.534	5.967	-0.678
9	107.737	27.330	0.924	1.414
10	206.449	96.460	6.256	-0.685
11	100.388	24.599	0.776	1.402
12	66.460	44.641	0.932	2.01

Utility Function Formulation. Before calculating confidence region utilities, the multiattribute utility function was formed. Using the survey results provided by the DOD (see Appendix A), four sets of one-dimensional utility values were obtained for both the eccentricity and area attributes. In addition, four responses for each attribute's scaling factor were also provided by the surveys.

TABLE 4

CIRCULAR CONFIDENCE REGION PARAMETERS

Geo. #	σ_x (n mi)	σ_y (n mi)	c	K	$A \cdot 10^4$n mi^2
1	310.491	263.629	.85	1.99498	120.538
2	44.055	21.555	.49	1.73329	1.832
3	246.329	89.501	.36	1.68904	54.383
4	51.324	35.124	.68	1.84833	2.827
5	340.604	63.637	.19	1.65637	99.992
6	119.730	23.132	.19	1.65637	12.356
7	30.022	24.574	.82	1.96656	1.095
8	122.943	100.264	.82	1.96656	18.364
9	49.632	14.811	.30	1.67383	2.168
10	79.755	70.105	.88	2.02341	8.182
11	46.157	13.757	.30	1.67383	1.875
12	29.396	22.972	.78	1.93059	1.012

One-dimensional utility functions were first fit to the survey data. These were obtained from plots of utility versus attribute value. For the eccentricity attribute, the four plots led to the creation of two distinct functional forms: 1) a piecewise linear function which served as an upper bound for the survey data; and 2) a power function representing a lower bound. The upper bound function consolidated the results from surveys #2 and #3 while the lower bound function was developed from survey #4 results. The plot of survey #1 was essentially contained

between these two bounding functions. As a result, these two functions bracketed the utility outcomes for the eccentricity attribute. The piecewise linear function consisted of three parts defined over the entire range of the eccentricity attribute:

$$\begin{aligned} U(X_{e1}) &= 1.143(X_e) && (0.0 \le e < 0.7) \\ U(X_{e1}) &= .8 && (0.7 \le e \le 0.9) \\ U(X_{e1}) &= 2(X_e) - 1 && (0.9 < e \le 1.0) \end{aligned} \quad (4)$$

The form of the lower bound function was obtained using nonlinear regression analysis:

$$U(X_{e2}) = 0.989(X_e)^{1.434} \quad (5)$$

Regarding the area attribute, the survey data was best described by a single linear function:

$$U(X_a) = -3.183 \cdot 10^{-5}(X_a) + 1.0 \quad (6)$$

The final parameters needed to form the multiattribute utility function were the attribute scaling factors k_e and k_a. For eccentricity, the surveys generated k_e values of 0.6, 0.5, 0.6, and 0.5. For the area attribute, survey responses of 0.8, 0.8, 0.8, and 0.5 were given for k_a. The results were synthesized to single values of k_e=0.55 and k_a=0.725 by averaging the above survey results.

Two multiattribute utility functions of the general form given by Eq (2) were developed:

$$U(X_{e1},X_a) = 0.55(U(X_{e1})) + 0.725(-3.183\times10^{-5}(X_a) + 1.0) - 0.275(U(X_{e1})) \cdot (-3.183\times10^{-5}(X_a) + 1.0) \quad (7)$$

where $U(X_{e1})$ may be any of the three functions given by Eq (4), and

$$U(X_{e2},X_a) = 0.55(0.989(X_e)^{1.434}) + 0.725(-3.183\times10^{-5}(X_a) + 1.0) - 0.275(0.989(X_e)^{1.434}) \cdot (-3.183\times10^{-5}(X_a) + 1.0) \quad (8)$$

Multiattribute Utility Calculations. Utility results for each of the 12 geolocations are presented in Tables 5 and 6. Table 5 values were calculated from the utility function defined by Eq (7) while Table 6 presents the outcomes from Eq (8). Table 6 only presents utility results for each confidence region, as the eccentricity and area attribute values are identical to the ones shown in Table 5. While the calculation is not shown, the eccentricity values for the elliptical confidence regions were calculated directly from the r_{max} and r_{min} values found in Table 3.

Utility Comparisons. In order to determine confidence region preferences, the magnitude of the difference between each region's utility was measured. The percent of utility lost when using the circular confidence region was

calculated using the left hand side of Eq (3). These results are presented in Table 7. Since the two multiattribute utility functions produced similar results for the attribute ranges of the 12 geolocations, only the results from the first function, Eq (7), are shown.

TABLE 5

MULTIATTRIBUTE UTILITY RESULTS FROM EQ (7)

	Elliptical Conf. Region			Circular Conf. Region		
#	X_e	$X_a \cdot 10^4$n mi	Utility	X_e	$X_a \cdot 10^4$n mi	Utility
1	.9965	19.736	.5462	0.0	120.538	0.0
2	.8734	1.370	.725	0.0	1.832	.302
3	.9949	9.947	.5444	0.0	54.383	0.0
4	.8789	2.175	.595	0.0	2.827	.073
5	.9993	6.462	.5492	0.0	99.992	0.0
6	.9906	2.882	.577	0.0	12.356	0.0
7	.8148	0.945	.793	0.0	1.095	.472
8	.9857	5.967	.5343	0.0	18.364	0.0
9	.9673	0.924	.844	0.0	2.168	.225
10	.8841	6.256	.44	0.0	8.182	0.0
11	.9695	0.776	.868	0.0	1.875	.292
12	.7408	0.932	.795	0.0	1.012	.491

TABLE 6

MULTIATTRIBUTE UTILITY RESULTS FROM EQ (8)

	Elliptical Region	Circular Region
#	Utility	Utility
1	.541	0.0
2	.731	.302
3	.540	0.0
4	.606	.073
5	.543	0.0
6	.574	0.0
7	.771	.472
8	.533	0.0
9	.847	.225
10	.456	0.0
11	.870	.292
12	.739	.491

TABLE 7

% OF UTILITY LOST BY USE OF THE CIRCULAR CR

Geo. #	% Loss
1	100
2	58
3	100
4	88
5	100
6	100
7	40
8	100
9	73
10	100
11	66
12	38

IV. A Likelihood Approach to Confidence Region Shape

This chapter presents both the approach used in conducting Phase II of the research effort and the results obtained. As to methodology, the initial conditions of this phase are presented first followed by a description of the formulated model.

Research Baseline In Phase I, the established geolocations contain bearings which all pass through the true transmitter location and therefore have a common point of intersection. In a more realistic case, the selected HFDF stations may in fact provide lines of-bearing (LOB) which do not intersect at a point common to all. It is still assumed, however, that each LOB is normally distributed with a mean, μ and standard deviation, σ. It is this case to which Phase II is addressed.

Model Formulation In order to determine the shape of a confidence region in the operational case, the following was devised. As discussed below, a grid was established containing both bearings from a number of HFDF receivers and a transmitter whose position was discretely moved throughout the grid.

Various test configurations were developed to examine the effects of sensor location, bearing angle, and bearing standard deviation on the confidence region shape. These configurations are detailed in Table 8 where the entries for

each sensor site are of the form: (station latitude (deg), station longitude (deg), bearing (deg measured CW from north), bearing σ (deg)).

TABLE 8

SAMPLE SENSOR CONFIGURATIONS

	Geolocation Sensor Site #			
Case #	1	2	3	4
A	(0,0,90,20)	(85,90,180,20)	-----	-----
B	(-45,45,45,20)	(85,90,180,20)	-----	-----
C	(45,45,135,20)	(85,90,180,20)	-----	-----
D	(0,0,90,20)	(85,90,180,20)	(-45,45,45,20)	-----
E	(0,0,90,20)	(85,90,180,20)	(-45,45,30,20)	-----
F	(0,0,90,20)	(85,90,180,20)	(-45,45,60,20)	-----
G	(0,0,90,20)	(-45,45,30,20)	(-45,135,-30,20)	-----
H	(0,0,90,10)	(-45,45,30,10)	(-45,135,-30,10)	-----
I	(0,0,90,20)	(-30,60,30,20)	(-30,120,-30,20)	-----
J	(0,0,90,20)	(85,90,180,20)	(-45,45,30,20)	(-45,135,-30,20)

Test cases A through C contain only two sensors and were designed to verify that, in fact, an elliptical region was produced since intersection at only one location was guaranteed. Also, cases B and C considered the effects of having both a sensor closer to the intersection point and bearings which were not perpendicular. Cases D through I contain three sensors each. Case D was designed with a common point of intersection in order to once again verify that an elliptically-shaped region would be produced. Cases

E and F varied the bearing of sensor #3 to possibly introduce distortions and/or multiple modes into the likelihood region. For all cases discussed so far, bearing standard deviation was set at 20 degrees. Cases G and H had configurations in which no two bearings were perpendicular to each other and bearing standard deviations were set to 20 and 10 degrees respectively. It was thought that reducing the bearing standard deviation would produce multiple modes within the area enclosed by the bearings. Case I examined the influence of sensor proximity to the point of intersection by placing sensors 2 and 3 closer to the intersection than in previous cases. This case was expected to have an effect similar to that of case H by not allowing the distance necessary for the bearing $\pm\sigma$ lines to become parallel, thereby failing to maximize the bearing likelihood. Finally, case J examined four sensors with a design similar to that of case E. By having three bearings intersect at a common point somewhat removed from the other intersection points, a multi-modal likelihood region was anticipated.

For each test case, a likelihood of obtaining each bearing given a discrete transmitter location was calculated assuming the bearing to be normally distributed with $\mu = 0$ and standard deviation σ. Code was developed which calculated the angular difference between the sensor bearing

line and the line connecting the transmitter and sensor locations. This angular difference represents a deviation from the bearing mean and permitted calculation of the bearing likelihood given the specific transmitter location. Since the bearings were assumed to be independent of each other, the joint probability or likelihood of obtaining all bearings is simply the product of the individual bearing likelihoods. Similar calculations made for all of the discrete transmitter locations within the grid. By moving the transmitter location throughout the grid, an un-normalized likelihood surface was obtained for each sensor configuration. The most likely position of the transmitter can be obtained from the coordinates of the mode. A plot of equal likelihood contours through this surface provides an indicator of the confidence region shape. FORTRAN and SAS source code written to perform the above likelihood manipulations and produce the plots are provided in Appendix C.

Results The plots obtained from SAS for each of the referenced cases are provided in Appendix D. The first plot for each case represents the likelihood surface. The second plot depicts equal probability contours through the likelihood surface.

Interesting results were seen for the test cases. For case A, a perfectly elliptical region was obtained, as

expected. Cases B and C were clearly much less elliptical, however. Bearings which are not perpendicular to one another result in equal probability contours with major axes tilted somewhat from those observed with perpendicular bearings. In both cases, the major axes were more oriented and curved toward the bearings from sensor #1. Another interesting feature for cases B and C was the thinner appearance of the contours.

The three and four bearing designs of cases D through J tended to result in nearly elliptical likelihood regions. For the common intersection of the three bearings in case D, nearly-perfect elliptical regions were generated. The distortions expected in cases E and F did not materialize. Only the orientation of the near elliptical regions changed as a function of the bearing from sensor #3. The removal of the 90 degree bearing in cases G through I tended to shift the near elliptical regions to the right (more positive latitude). The reduction in bearing standard deviation to 10 degrees in case H effectively concentrated the likelihood but failed to produce multiple modes within the area. Subsequent attempts to use values of standard deviation less than 10 degrees failed to produce SAS output. This was due to the extremely small likelihood values obtained with $\sigma <$ 10 degrees. By scaling down the area covered by the resulting bearing intersections, bearing standard deviations

of less than 10 degrees could be evaluated. Case I results showed little effect from the relatively close setting of sensors 2 and 3. The likelihood regions exhibited near elliptical behavior except for the outermost contour line. Lastly, the only four bearing design, case J, exhibited near elliptical likelihood regions which were shifted to more positive latitudes despite the reinsertion of the 90 degree bearing. This was most likely due to the intersection of three bearings in a north latitude.

V. Conclusions and Areas for Further Research

Conclusions Discussion of the results from this research is done at two levels. First, general conclusions from both phases are presented. It is here where the attempt is made to tie together Phase I and II results. The second level interprets Phase I results in terms of confidence region shape preferences.

The following general conclusions are supported by this research.

1. For the utility function formulations represented by Eqs (7) and (8), the utility of a geolocation's elliptical confidence region was always superior to the utility of its' corresponding circular region. As observed from Tables 5 and 6, there was little difference in the utility values calculated from the two formulations. In general, the dominance of the elliptical confidence region is bounded by a factor of 1.3 in the worst case and unbounded in the best case.
2. Overall, Phase II results indicated that for the cases tested, it appears reasonable to assume an elliptical shape for the confidence region of geolocations with multiple points of bearing intersection.

Given these individual conclusions reached by Phase I and II respectively, it appears that the confidence region of an

operationally established geolocation can be approximated by an analytically derived elliptical region centered on the most likely transmitter position. This approach is addressed in the recommendations as a potential follow-on to this research.

On the basis of Phase I results, the determination of whether to prefer the elliptically-shaped confidence region or its equal probability circular region is not nearly as straightforward as it appears at first glance.

To understand why, attention is directed first to those geolocations which result in confidence region areas less than the critical area, A_c , of 3.142×10^4 n mi^2 . It is these geolocations which could be accepted under current DOD practice. From the 12 geolocations, samples 2, 4, 7, 9, 11, and 12 fall into this acceptance category. From Table 7, the percent of utility lost by using the circular confidence region for these geolocations ranges from 38% to 88%. With these values, the dominance of the elliptical region appears obvious. However, the plots for these same geolocations in Appendix B do not support this dominance in all cases.

An explanation can be given to explain this apparent ambiguity. As the circular confidence region area approaches A_c , the elliptical region will appear "infinitely" better than its circular counterpart. This phenomenon is a result of the utility function formulation,

as was discussed. Therefore, the percent loss value in Table 7 should not be viewed as an absolute measure of difference between the two regions. For example, the elliptical region of geolocation 4 (circular region area of 2.827×10^4 n mi^2) has 88% more utility than its corresponding circular region. This difference is the highest among the six geolocations in the acceptance category. But when comparing the traces of these six geolocations, the elliptical regions of geolocations 9 and 11, with utility advantages of 73% and 66%, respectively, appear to have much more value than the elliptical region in geolocation 4. As a result, true confidence region distinctions should only be based on Table 7 results when the area of the circular confidence region is much less than A_c, as is the case with geolocations 2, 7, 9, 11, and 12. It is from these utility loss percentages that the DOD can establish its threshold percentage, δ, representing the minimum loss percentage required to use the elliptical confidence region in performing SAR analyses on the North Sea transmitter area.

Regarding the remaining geolocations, all would presently be rejected because their circular confidence region areas are greater than A_c . Sample 6, however, was unique in that it had a corresponding elliptical area less than the critical value. The dominance of the elliptical region for this sample is clearly shown in Appendix B and

indicates that a false rejection would have occurred. Samples 1, 3, 5, 8, and 10 had both elliptical and circular confidence region areas greater than A_c . Any utility in these geolocations was a direct result of the eccentricity of the elliptical region. Four out of these five geolocations had elliptical confidence regions with very high eccentricities (> 0.98) perhaps warranting reconsideration of geolocation rejection based solely on area.

Areas for Further Research Several possibilities exist for further research in HFDF confidence region analysis.

1. The development of the utility function was based on questionnaire responses from the analytical community only. Views from the operational community must also be sought and somehow incorporated in order to arrive at a more representative utility function. Further, the setting of the threshold percentage δ is likely to vary depending on the user community questioned. The dynamics of this situation warrant additional work in the area of confidence region preference. In addition, refinement of the utility function formulation should be accomplished by seeking out other confidence region criteria (attributes) and by adjusting the ranges of values used for the present attributes. An example of the latter could be adjusting the eccentricity range to

be from 0.5 to 1 thereby assigning considerably less utility to more circular-like regions.

2. The sample space should be extended to include other SAR transmitter areas of interest and the results applied to establish desirable subsets of HFDF sites for each transmitting area. Application of these results to the refinement of optimal frequency assignments should also be investigated.

3. Using bearing test data from operational geolocations, the feasibility of establishing analytical confidence region approximations can be investigated using the following methodology: 1) locate the most likely transmitter position (the mode of the likelihood surface) using *some* type of gradient search technique; and 2) generate an analytical confidence region centered on this estimate by placing all of the test bearings through this location. Also, validation of these confidence regions can be explored by creating a multi-variate normal distribution which models this real world situation.

Appendix A: Utility Function Input Data

Questionnaire

Answers to the following sets of questions will permit development of a Keeney-Raiffa multiattribute utility function for HFDF confidence areas. This utility function will be used to determine preferences between elliptical confidence regions (as developed by D7 Technical Memorandum No. 72-05) and equivalent probability circular approximations to these regions.

The first two sets of questions below will permit measurement of the utility of each attribute or dimension individually. The two attributes used in this research are the eccentricity, e, and area, A, of the confidence region. Eccentricity is a measure of the shape of an elliptical region and varies in value between 1 (most desired) and 0 (least desired). The figure below illustrates ellipses having the same major axis but different eccentricities.

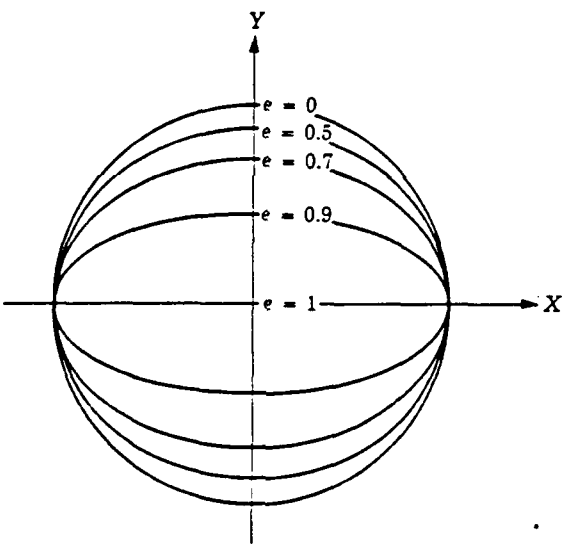

Figure 2. Illustration of Ellipse Eccentricity (5:102)

The area of the confidence region will vary in value from near 0 (most desired) to πd_i^2 (least desired) where d_i is the maximum allowable error radius in NM. Prior to answering the questions relating to the area attribute, the respondent must identify below the largest existing d_i value which will be used

throughout the questionnaire.

d_i - 100 NM

1) One-Dimensional Attribute: Eccentricity

"If given the choice between either a 50:50 chance of getting an eccentricity, e, of 0.7 or 0.0 (see figure for approximate shapes), or a P:(1-P) chance of getting an eccentricity of 1 or 0, which would you prefer if P=40%? 10%? 30%? or finally, 20%?" (Sequentially answer these questions until a probability is reached where you are indifferent between the two choices and provide that value below.)

P = _____

Answer these same questions above if the values of e in the first chance were now 0.5 or 0.0. Enter the new probability below.

P = _____

Answer these same questions above if the values of e in the first chance were now 0.9 or 0.0. Enter the new probability below.

P = _____

Answer these same questions above if the values of e in the first chance were now 0.8 or 0.0. Enter the new probability below.

P = _____

2) One-Dimensional Attribute: Area

"If given the choice between either a 50:50 chance of getting an area, A, of $0.5(\pi(d_i)^2)$ or $\pi(d_i)^2$, or a P:(1-P) chance of getting an area of near 0 (point location) or $\pi(d_i)^2$, which would you prefer if P=40%? 10%? 30%? or finally 20%?" (Sequentially answer these questions until a probability is reached where you are indifferent between the two choices and provide that value below.)

P = _____

Answer the same questions if the values of A in the first chance were now $.25(\pi(d_i)^2)$ or $\pi(d_i)^2$. Enter the new probability below.

P = _____

Answer the same questions if the values of A in the first chance were now $.75(\pi(d_i)^2$ or $\pi(d_i)^2$. Enter the new probability below.

P = _____

The next two sets of questions will allow calculation of the scaling factors for each attribute. Each factor, k_i, represents the multiattribute utility of the best level of the attribute i when all other attributes are at their worst levels.

3) Scaling Factor: Eccentricity

"Suppose you know that you could certainly obtain a geolocation X which had the characteristics $(e \approx 1, A = \pi d_i^2)$. You could also establish a geolocation that with a probability P will have $(e \approx 1, A \approx 0)$ or which, with probability (1-P) might have $(e = 0, A = \pi d_i^2)$. Would you opt for geolocation X if P=90%? 10%? 80%? 20%? 70%? 30%? 60%? 40%? or finally 50%?"

Enter the probability value below for which you would opt for geolocation X.

P = _____

4) Scaling Factor: Area

"Suppose you know instead that you could certainly obtain a geolocation Y which had the characteristics $(A \approx 0, e = 0)$. You could also establish a geolocation that with a probability P will have $(e \approx 1, A \approx 0)$ or which, with probability (1-P), might have $(e = 0, A = \pi d_i^2)$. Would you opt for geolocation Y if P=90%? 10%? 80%? 20%? 70%? 30%? 60%? 40%? or finally 50%?"

Enter the probability value below for which you would opt for geolocation Y.

P = _____

Thank you for your assistance in completing this questionnaire. Please return it to the address shown below not later than 30 Nov 90.

Capt Paul Nemec
AFIT/ENA
P.O. Box 4574
Wright-Patterson AFB, OH 45433-6583

Questionnaire Responses

Tables 9 and 10 each provide four sets of responses to the above questionnaire. Table 9 contains results for the eccentricity attribute while Table 10 lists area attribute values. Scaling factor results for both attributes appear in Chapter III.

TABLE 9

ECCENTRICITY ATTRIBUTE SURVEY RESULTS

Survey #	(X_e, P)	$U(X_e)$
1	(.7,.3)	.6
	(.5,.2)	.4
	(.9,.4)	.8
	(.8,.4)	.8
2	(.7,.4)	.8
	(.5,.3)	.6
	(.9,.4)	.8
	(.8,.4)	.8
3	(.7,.4)	.8
	(.5,.3)	.6
	(.9,.4)	.8
	(.8,.4)	.8
4	(.7,.29)	.58
	(.5,.19)	.38
	(.9,.42)	.84
	(.8,.36)	.72

TABLE 10

AREA ATTRIBUTE SURVEY RESULTS

Survey #	$(X_a \cdot 10^4 \text{n mi}^2, P)$	$U(X_A)$
1	(1.571,.3)	.6
	(0.785,.4)	.8
	(2.356,.1)	.2
2	Same as for #1	Same as for #1
3	Same as for #1	Same as for #1
4	(1.571,.25)	.5
	(0.785,.38)	.76
	(2.356,.13)	.26

Appendix B: Confidence Region Plots

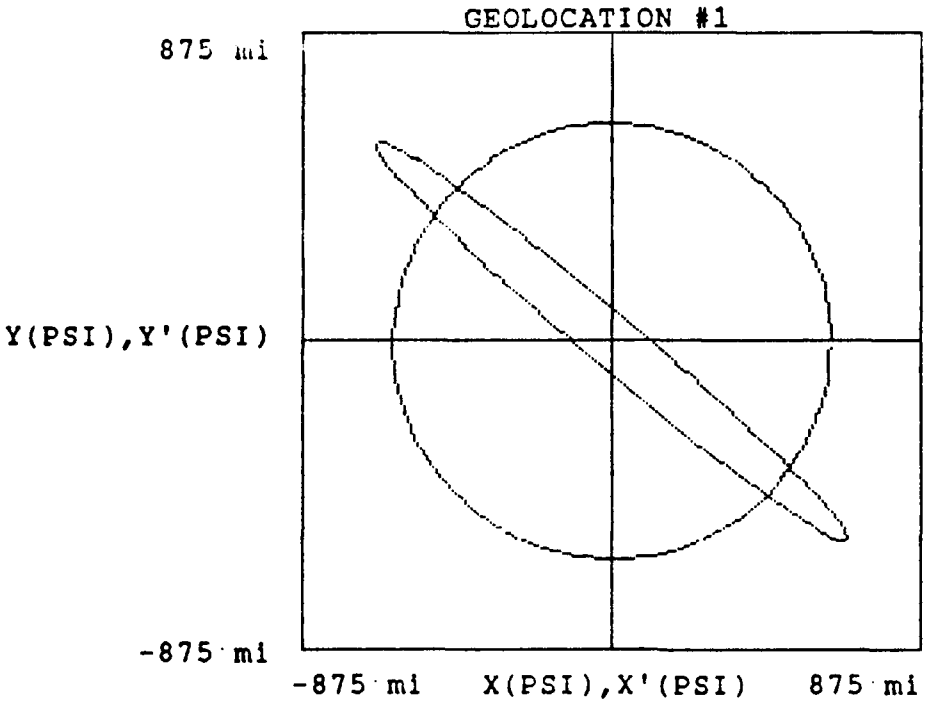

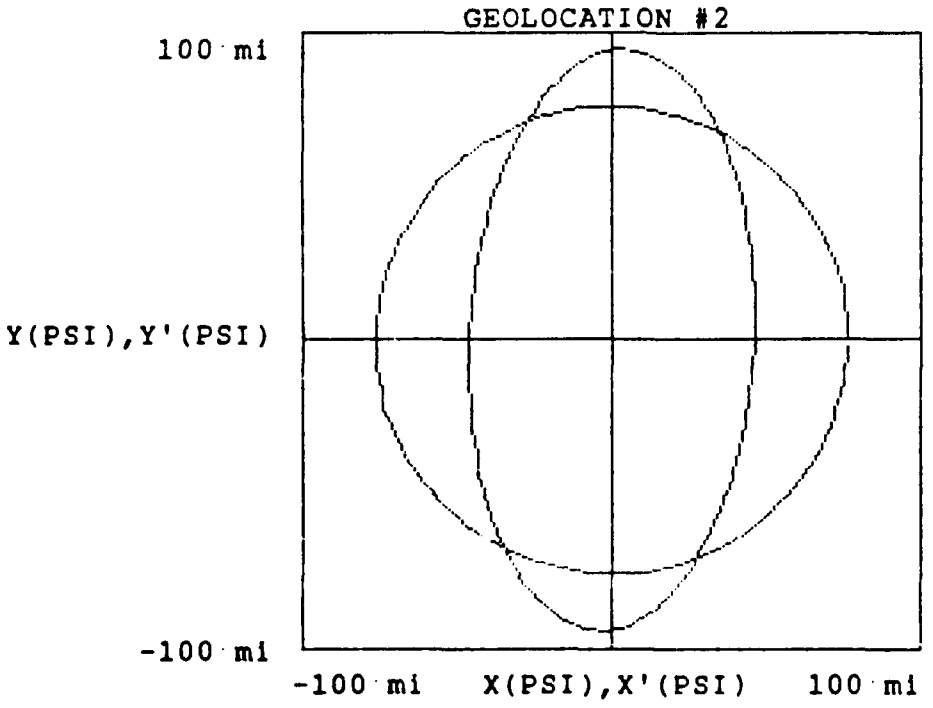

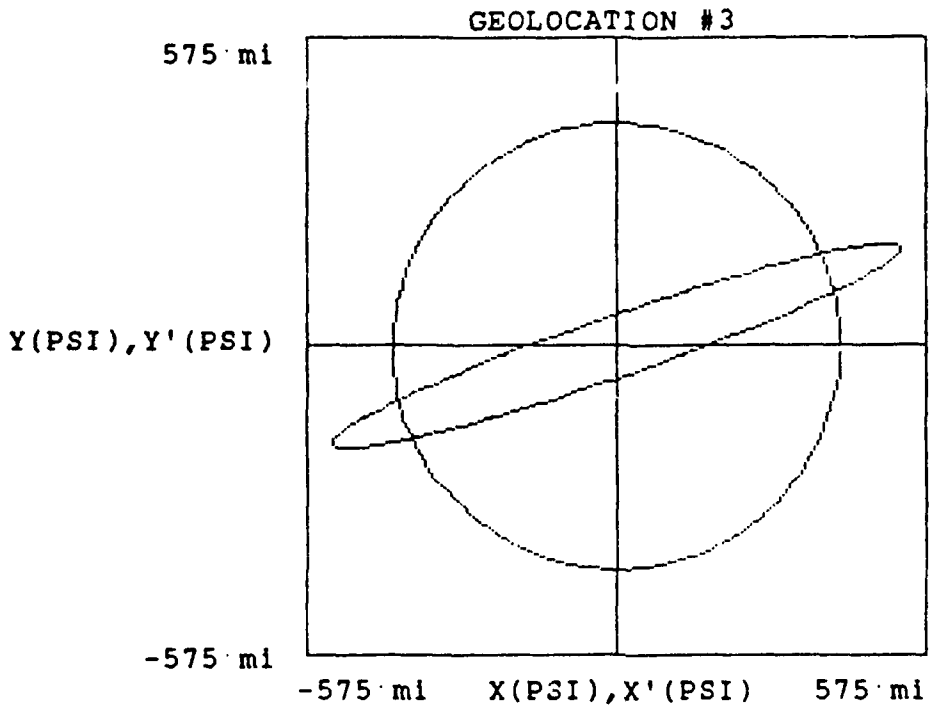
GEOLOCATION #3
575 mi
Y(PSI),Y'(PSI)
-575 mi
-575 mi
X(P3I),X'(PSI)
575 mi

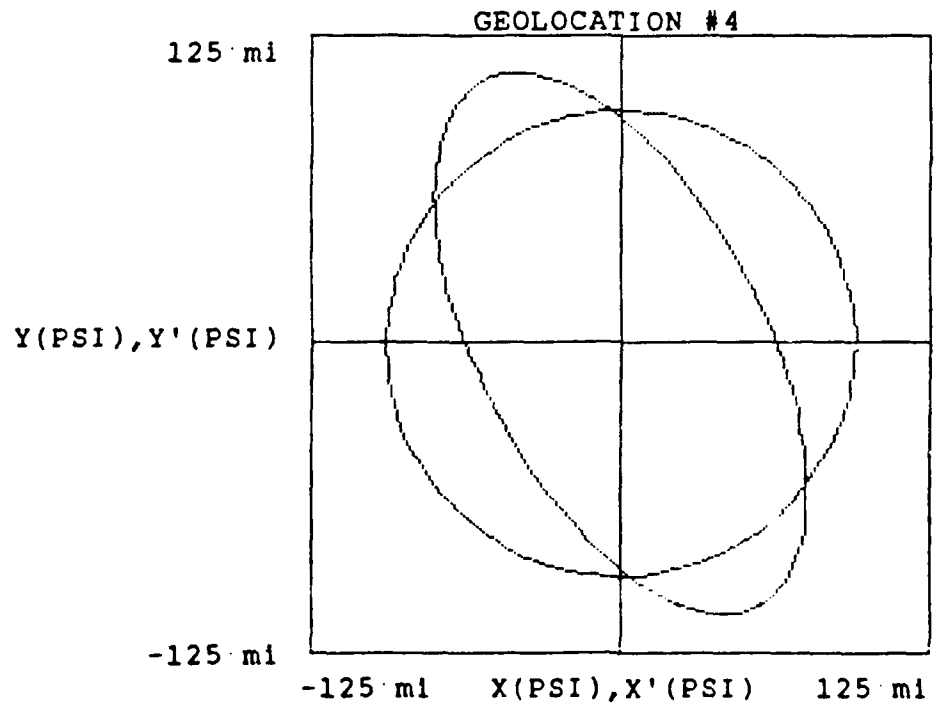
GEOLOCATION #4
125 mi
Y(PSI),Y'(PSI)
-125 mi
-125 mi
X(PSI),X'(PSI)
125 mi

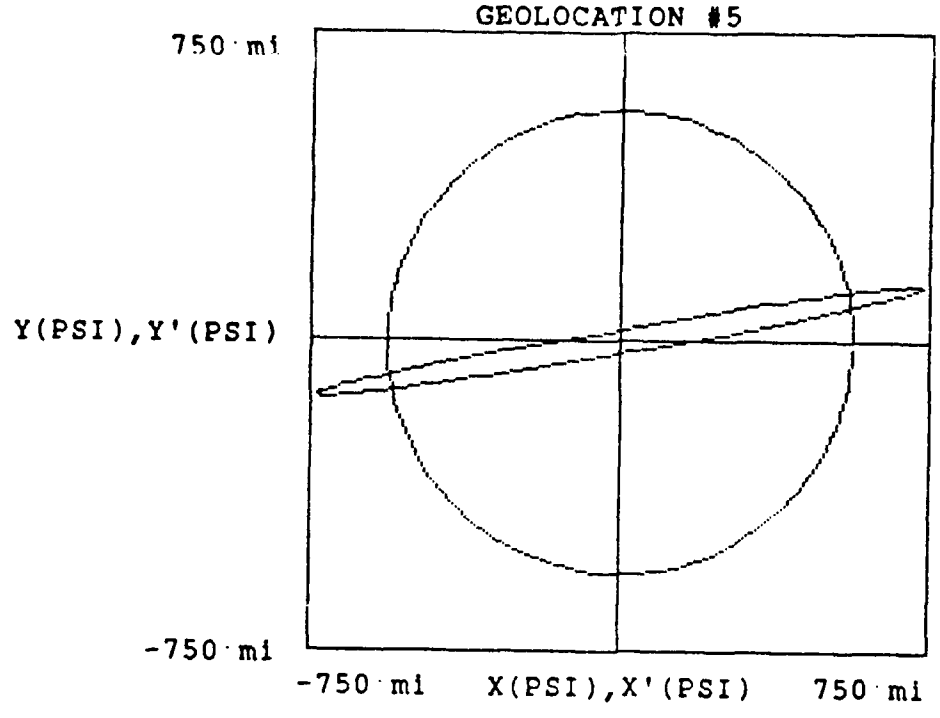
GEOLOCATION #5
750 mi
Y(PSI),Y'(PSI)
-750 mi
-750 mi
X(PSI),X'(PSI)
750 mi

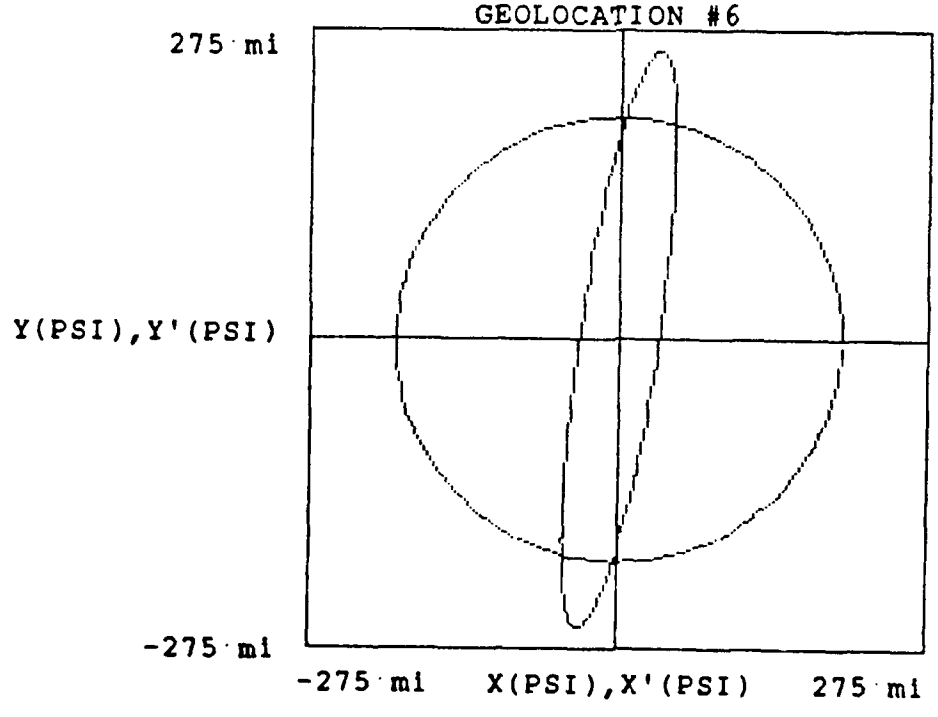
GEOLOCATION #6
275 mi
Y(PSI),Y'(PSI)
-275 mi
-275 mi
X(PSI),X'(PSI)
275 mi

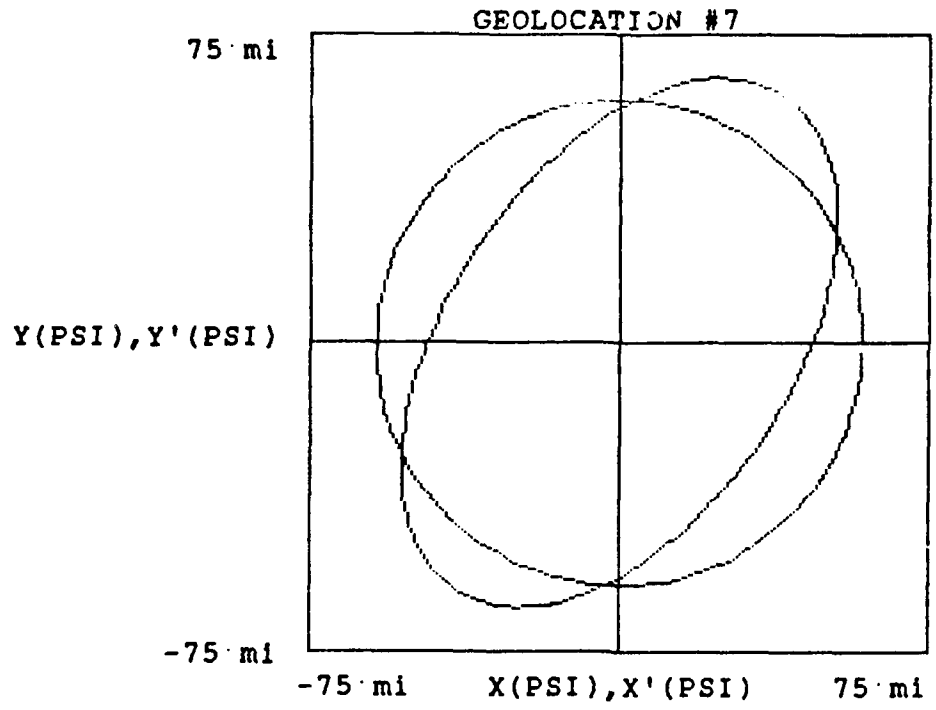
GEOLOCATION #7
75 mi
Y(PSI),Y'(PSI)
-75 mi
-75 mi
X(PSI),X'(PSI)
75 mi

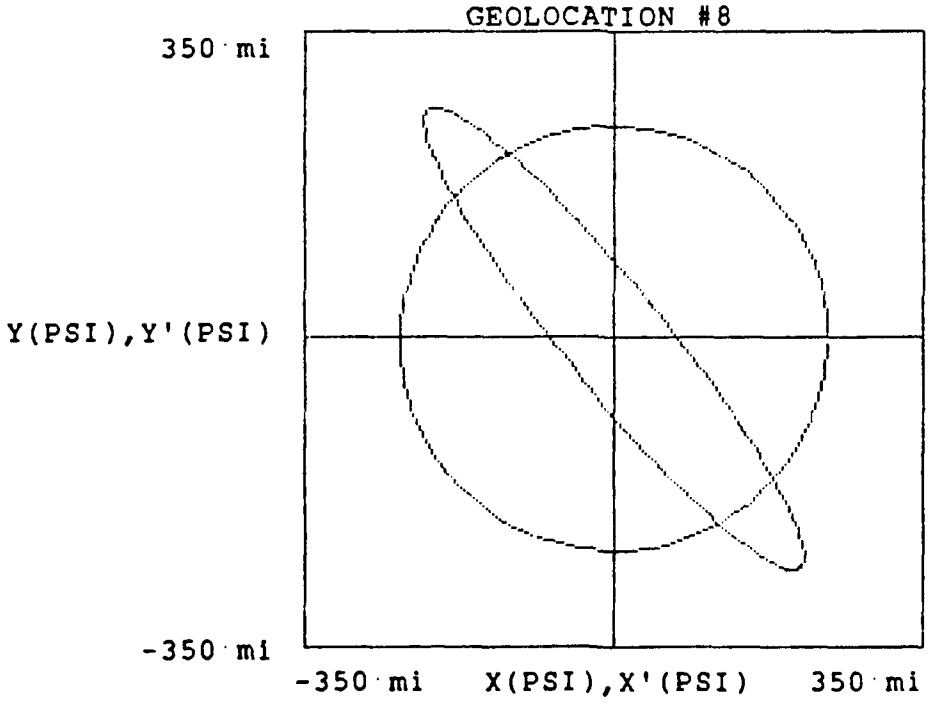
GEOLOCATION #8
350 mi
Y(PSI),Y'(PSI)
-350 mi
-350 mi
X(PSI),X'(PSI)
350 mi

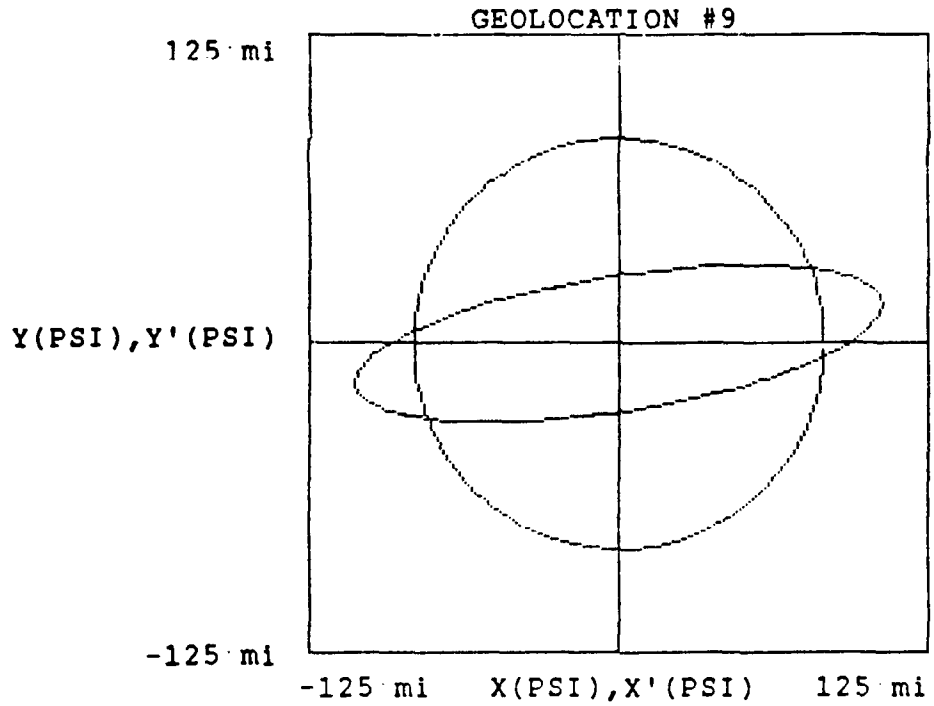
GEOLOCATION #9
125 mi
Y(PSI),Y'(PSI)
-125 mi
-125 mi
X(PSI),X'(PSI)
125 mi

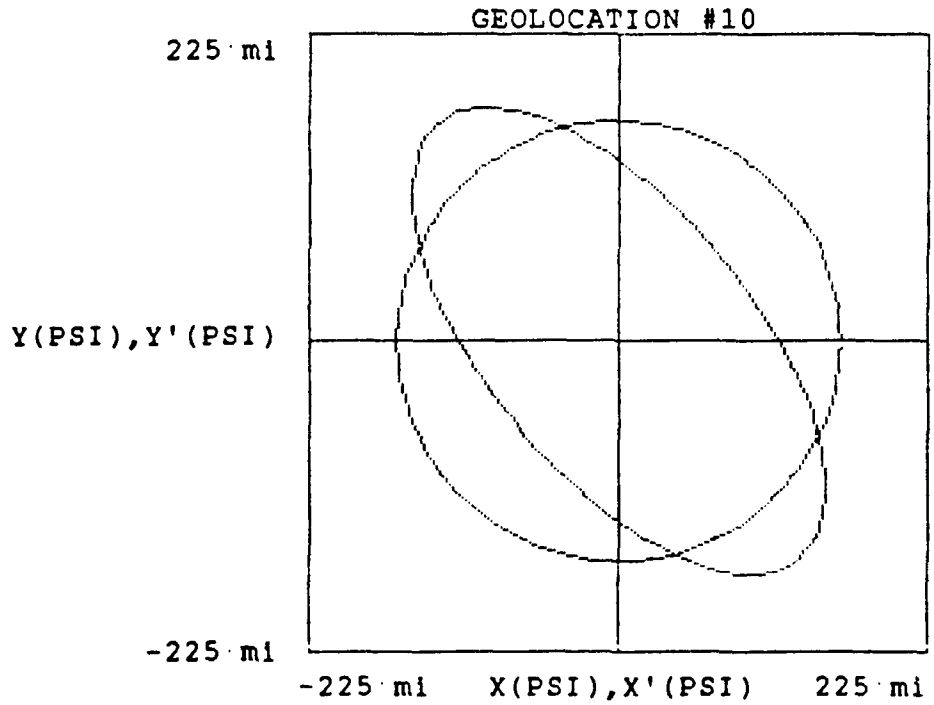
GEOLOCATION #10
225 mi
Y(PSI),Y'(PSI)
-225 mi
-225 mi
X(PSI),X'(PSI)
225 mi

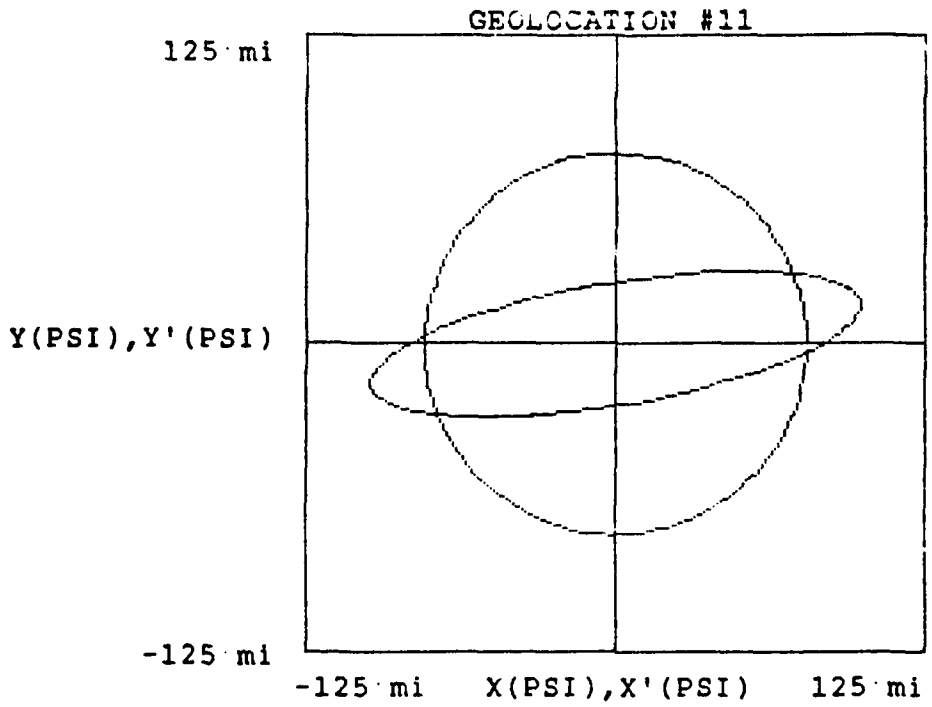
GEOLOCATION #11
125 mi
Y(PSI),Y'(PSI)
-125 mi
-125 mi
X(PSI),X'(PSI)
125 mi

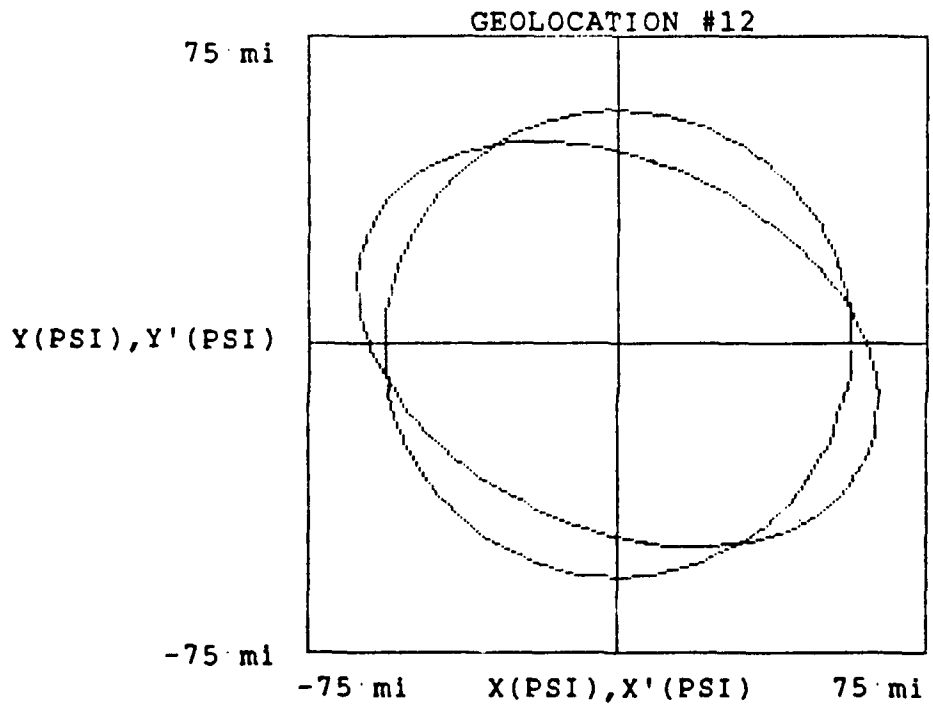
GEOLOCATION #12
75 mi
Y(PSI),Y'(PSI)
-75 mi
-75 mi
X(PSI),X'(PSI)
75 mi

Appendix C: Phase II FORTRAN and SAS Code

----- FORTRAN SOURCE -----

```
c
c The output file FORT.1 contains a (Lat,Lon,Likelihood) data set
c
      real Likely
      real LLat,LLon
      real LLLat, LLLon, URLat, URLon, DLat, DLon
      dimension Sensor(10,4)
      integer Lat,Lon,Azm,SDv
      data Lat/1/Lon/2/Azm/3/SDv/4/

      DegRad = ATAN(1.0)/45.0
      print *,'How many sensors? '
      read *, NS
      if (Ns.le.0) go to 20
      do 10 i = 1 , Ns
        print *,'Sensor ',i,'   Latitude, Longitude? '
        read *,Sensor(i,Lat),Sensor(i,Lon)
        print *,'Sensor ',i,'   Azimuth, Std dev? '
        read *,Sensor(i,Azm),Sensor(i,SDv)
 10     continue
      print *,'Lat, lon of lower left corner of target box? '
        read *,LLLat,LLLon
      print *,'Lat, lon of upper right corner of target box? '
        read *,URLat,URLon
      print *,'Latitude, longitude step sizes?'
        read *,DLat,DLon
        go to 30
 20   continue
        Ns = 3
        Sensor(1,Lat) =   0.0
        Sensor(1,Lon) =   0.0
        Sensor(1,Azm) =  90.0
        Sensor(1,SDv) =  10.0

        Sensor(2,Lat) =  85.0
        Sensor(2,Lon) =  90.0
        Sensor(2,Azm) = 180.0
        Sensor(2,SDv) =  10.0

        Sensor(3,Lat) = -20.0
        Sensor(3,Lon) =  60.0
        Sensor(3,Azm) =  45.0
        Sensor(3,SDv) =  10.0

        LLLat = -30.0
        LLLon =  60.0
        URLat =  30.0
        URLon = 120.0
        DLat = 2.0
        DLon = 2.0
```

```
 30   continue

 31   continue

      TLat = LLLat
c
c  repeat
  40  continue
        TLon = LLLon
c
c    repeat
  50    continue
          Likely = 1.0
          do 60 i = 1 , Ns
            Call Taraz(Sensor(i,Lat),Sensor(i,Lon),TLat,TLon,TAzm,TRng)
            AzmErr = ACOS(cos(DegRad*(TAzm-Sensor(i,Azm))))/DegRad
            Likely = Likely*Rormal(AzmErr,Sensor(i,SDv))
  60        continue
            write(1,1000)Tlat,TLon,Likely
 1000       format(1x,2f7.2,e16.5)
          TLon = TLon + DLon
c
c      until
          if ( TLon .le. URLon ) go to 50
        TLat = TLat + DLat
c    until
        if (Tlat .le. URLat ) go to 40

      end

      real function Rormal(Miss,StdDev)
      real Miss, StdDev
c     print *,'Miss =',Miss
c     print *,'    StdDev =',StdDev
      Rormal = exp(-(Miss*Miss/(2.0*StdDev*StdDev)))
c     print *,'    Normal =',Normal
      return
      end


      Real Function Sgn(X)
      IF (X.lt.0.0) Sgn=-1.0
      IF (X.eq.0.0) Sgn= 0.0
      IF (X.gt.0.0) Sgn= 1.0
      RETURN
      END
```

```
      Subroutine Taraz(Lt1,Ln1,Lt2,Ln2,Azimuth,Range)
C
C Subroutine Taraz will determine the surface range and azimuth from one
C point to another using great circle routes.
C
      Real Lt1, Ln1, Lt2, Ln2, Azimuth, Range
      Degrad = ATAN(1.0)/45.0
      T=SIN(Degrad*Lt1)*SIN(Degrad*Lt2)
     1  +COS(Degrad*Lt1)*COS(Degrad*Lt2)*COS(Degrad*(Ln2-Ln1))
      IF (ABS(T).gt.1.0) T=SGN(T)
      Range=ACOS(T)
      T=SIN(Range)*COS(Degrad*Lt1)
      IF (ABS(T).ge.0.0001)
     1  T=(SIN(Degrad*Lt2)-COS(Range)*SIN(Degrad*Lt1))/T
      IF (ABS(T).gt.1.0) T=SGN(T)
      Azimuth=ACOS(T)/Degrad
      Range=Range*3443.0
      IF (SIN(Degrad*(Ln2-Ln1)).lt.0.0) Azimuth=-Azimuth
      RETURN
      END
```

```
----- SAS -----

goptions device=tek4107;

data pdf;
infile normal;
input lt ln pr;

proc g3grid data=pdf out=graph;
  grid ln*lt=pr / partial
                  near = 8
                  axis1 = 45 to 105 by 5
                  axis2 = -30 to 30 by 5;

title1 f=xswiss ' ';
proc g3d data=graph;
  plot ln*lt=pr / caxis = white
                  ctext = white
                  ctop = green
                  cbottom = rose;
proc gcontour;
  plot ln*lt=pr;
  run;
```

Appendix D: Likelihood Surfaces and Contours

For Phase II sample sensor configurations A through J, the corresponding likelihood surfaces followed by their equal-probability contours are shown.

Case A

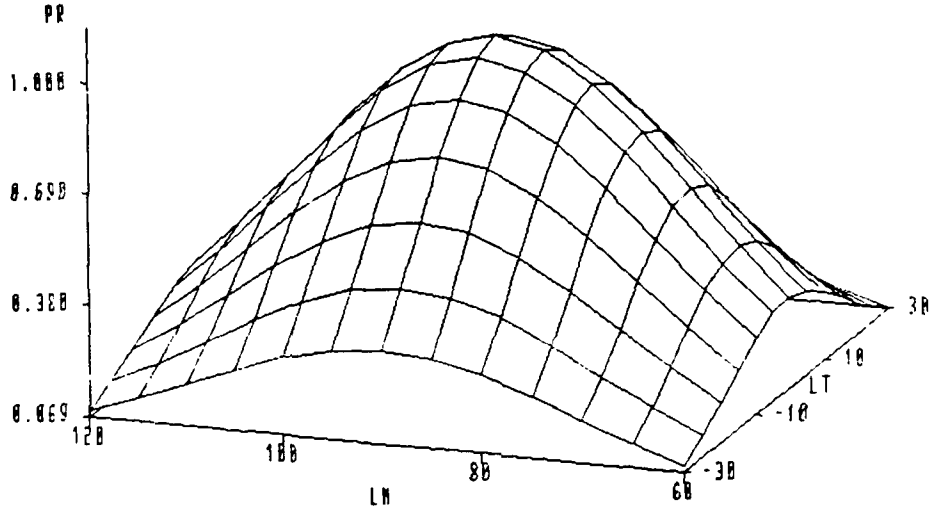

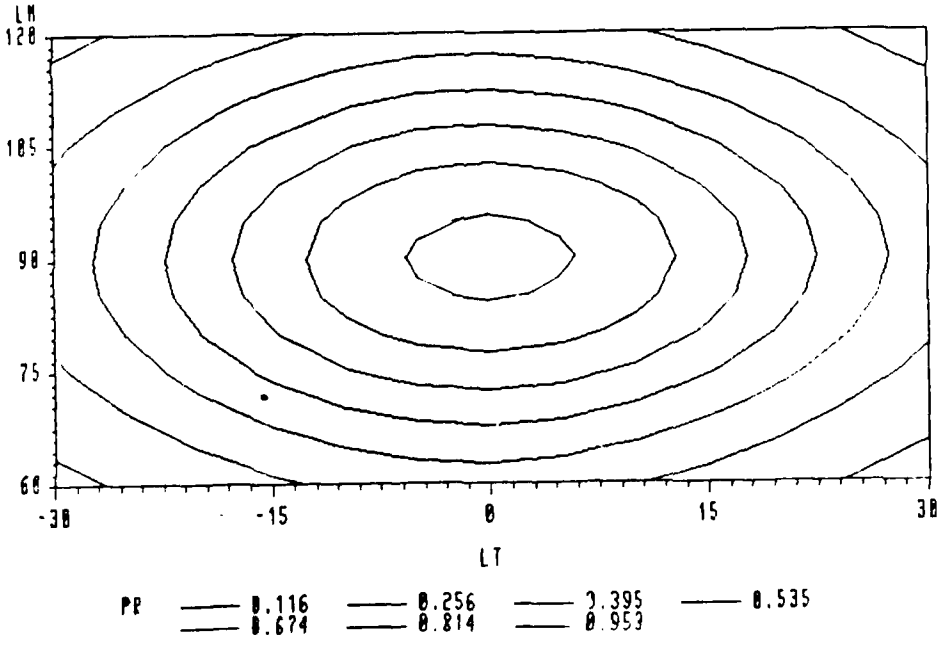

Case B

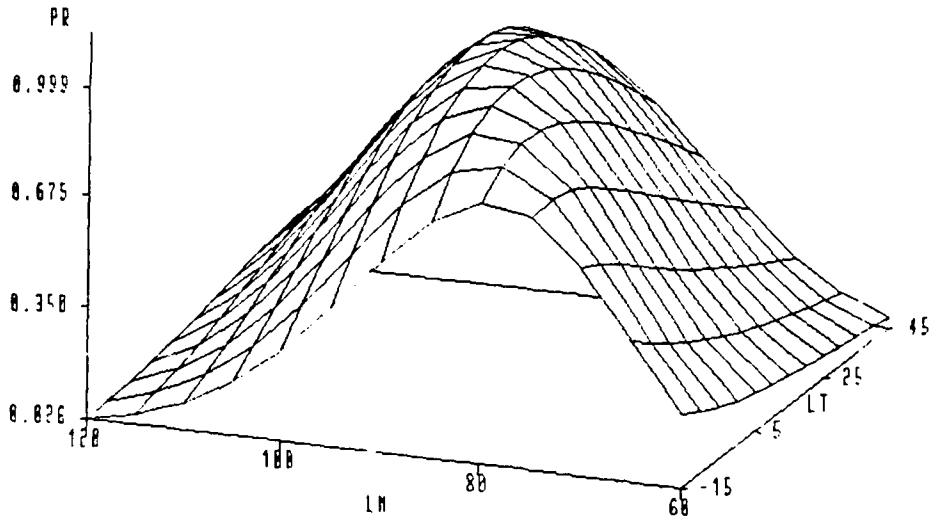
PR
0.999
0.675
0.350
0.026
120
100
80
60
LM
45
25
5
-15
LT

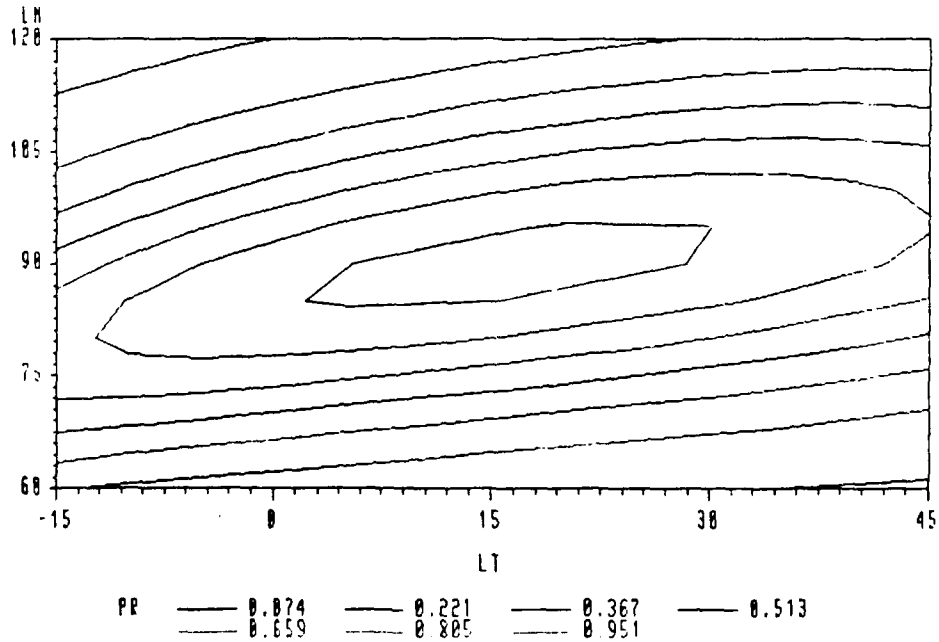
LM
120
105
90
75
60
-15
0
15
30
45
LT
PR
0.074
0.659
0.221
0.805
0.367
0.951
0.513

Case C

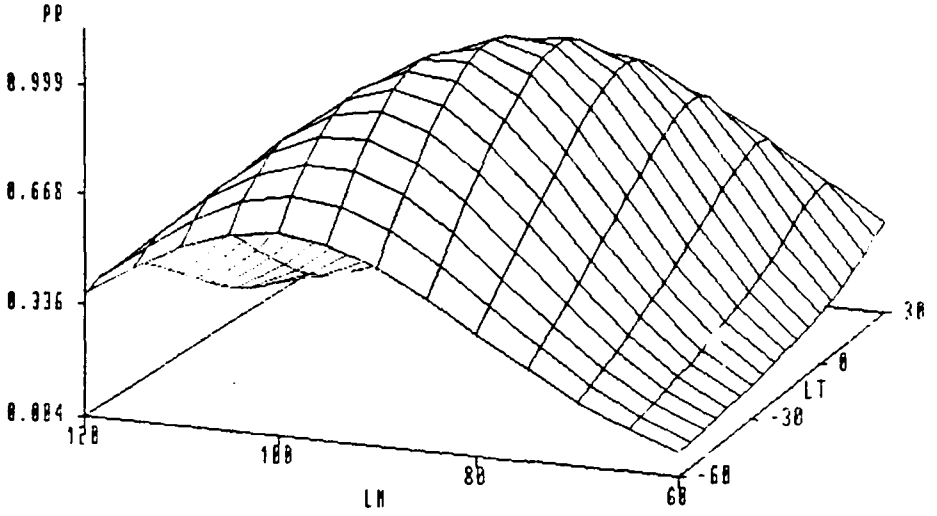
PR
0.999
0.668
0.336
0.004
120
100
80
60
LM
30
0
-30
-60
LT

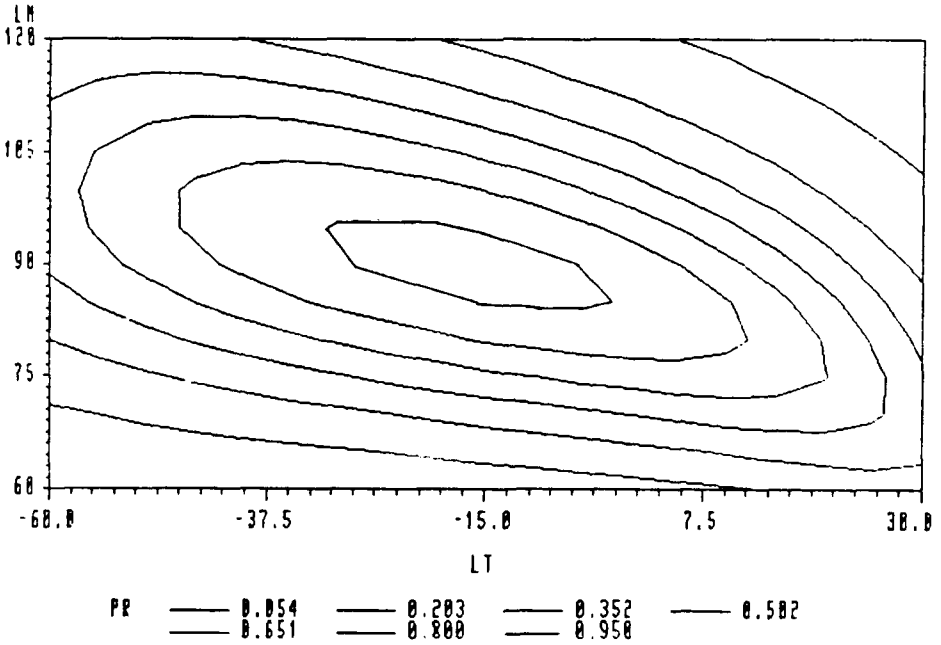
LM
120
105
90
75
60
-60.0
-37.5
-15.0
7.5
30.0
LT
PR
0.054
0.203
0.352
0.502
0.651
0.800
0.950

Case D

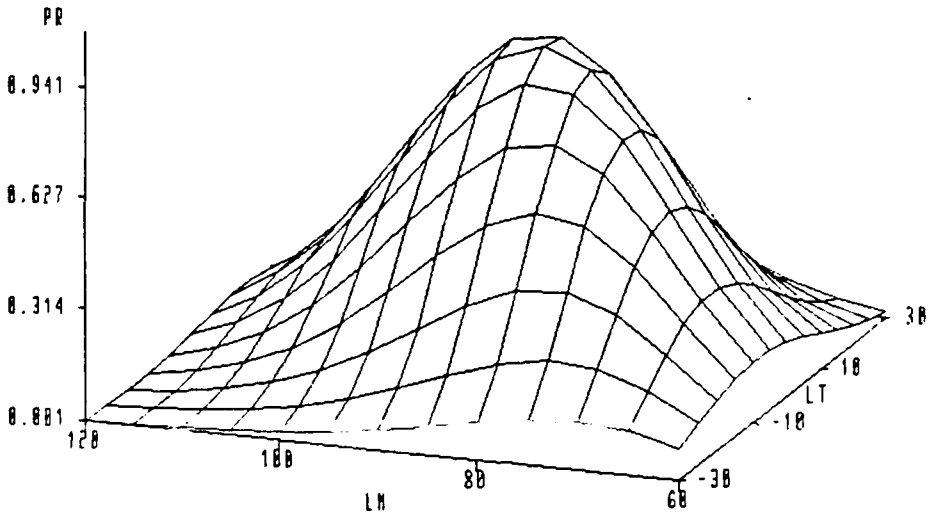
PR
0.941
0.627
0.314
0.001
120
100
80
60
LM
30
10
-10
-30
LT

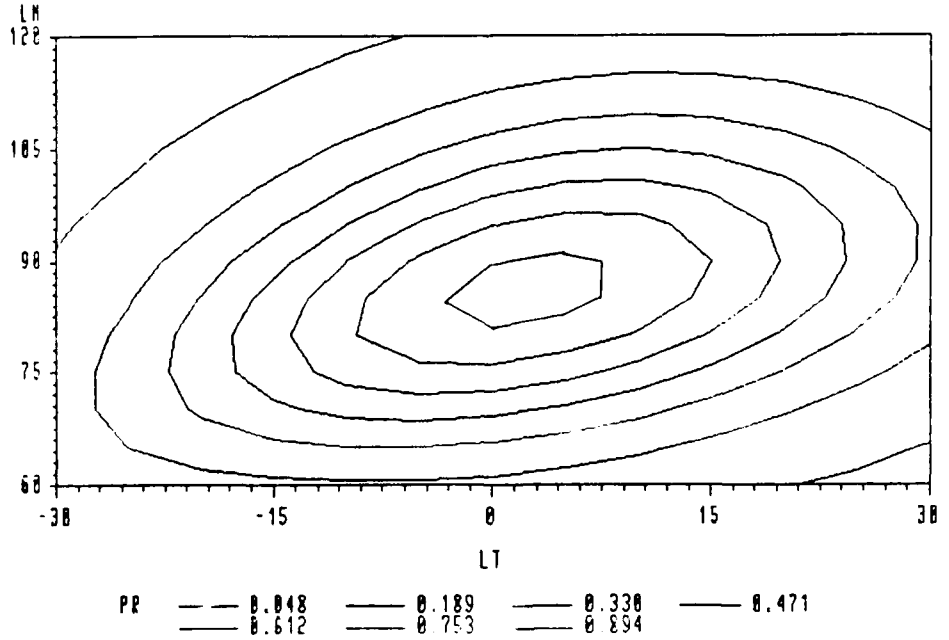
LM
120
105
90
75
60
-30
-15
0
15
30
LT
PR
0.048
0.189
0.330
0.471
0.612
0.753
0.894

Case E

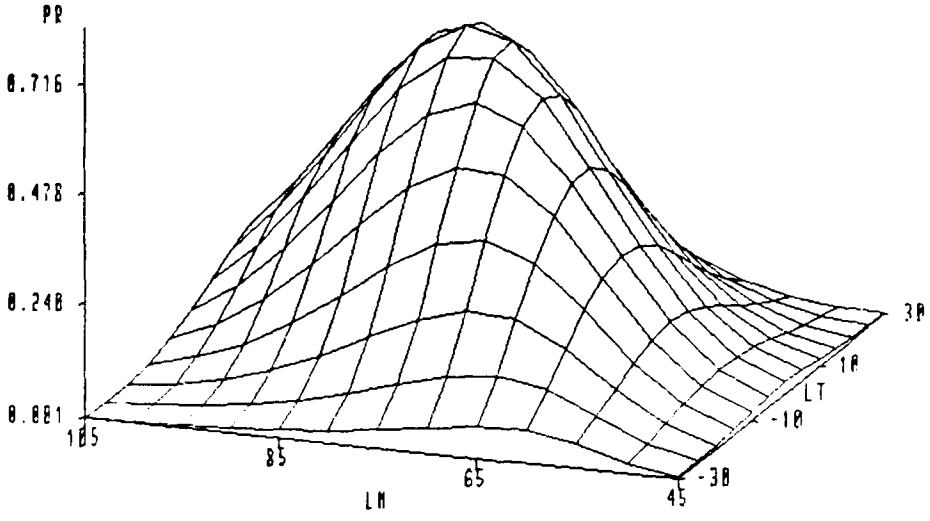
PR
0.716
0.478
0.240
0.001
105
85
65
45
LM
30
10
LT
-10
-30

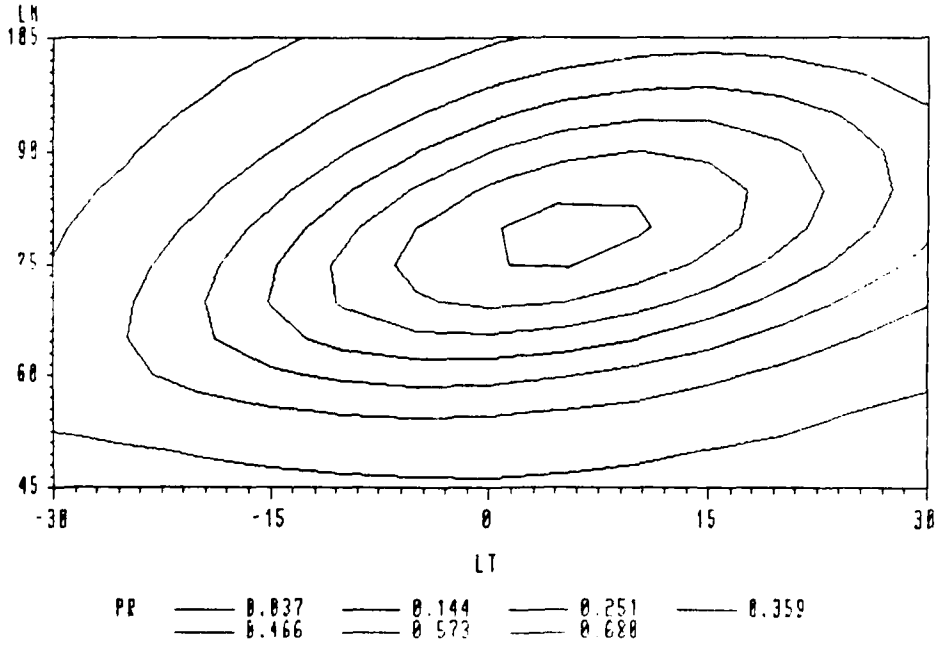
LM
105
90
75
60
45
-30
-15
0
15
30
LT
PR
0.037
0.144
0.251
0.359
0.466
0.573
0.680

Case F

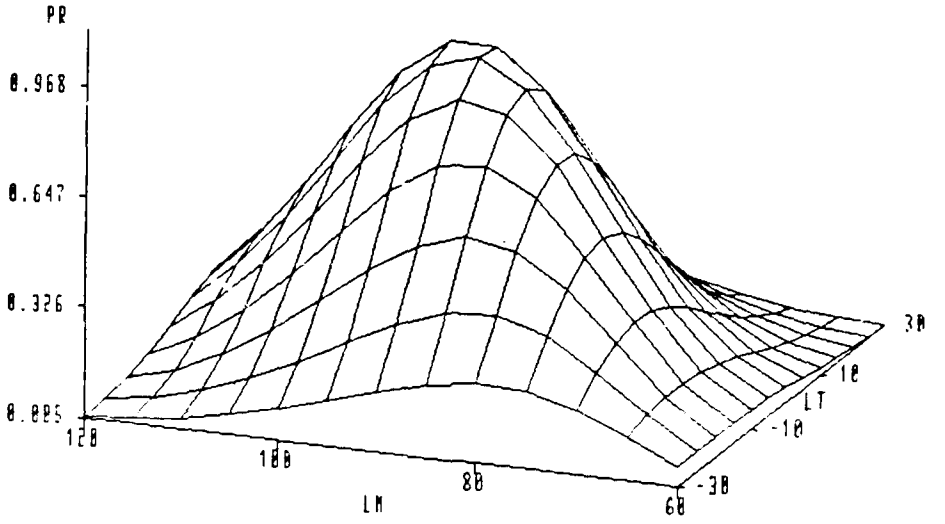
PR
0.968
0.647
0.326
0.005
120
100
80
60
LM
30
10
-10
-30
LT

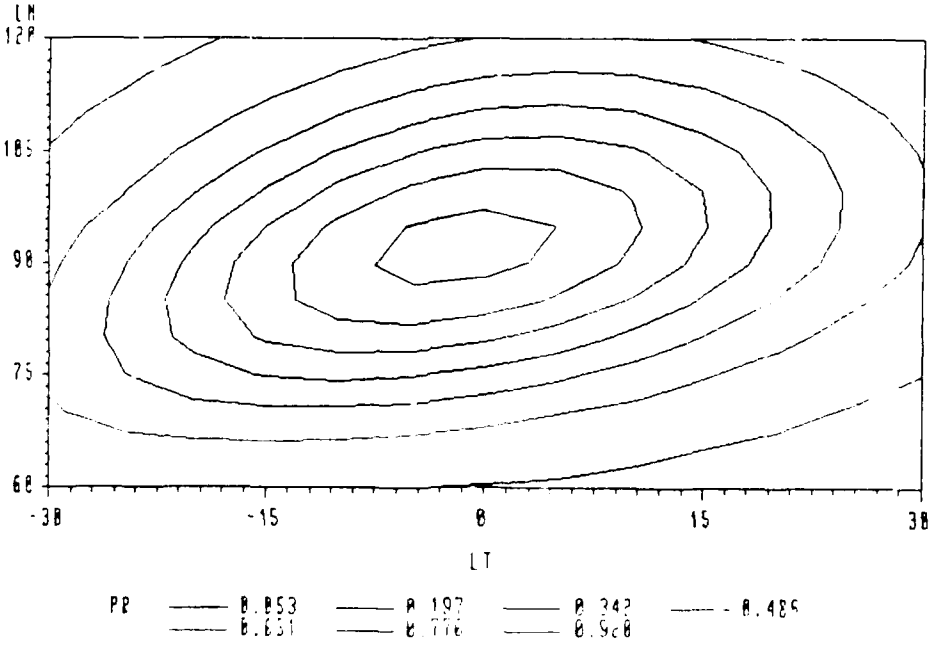
LM
120
105
90
75
60
-30
-15
0
15
30
LT
PR
0.853
0.631
0.197
0.776
0.342
0.920
0.485

Case G

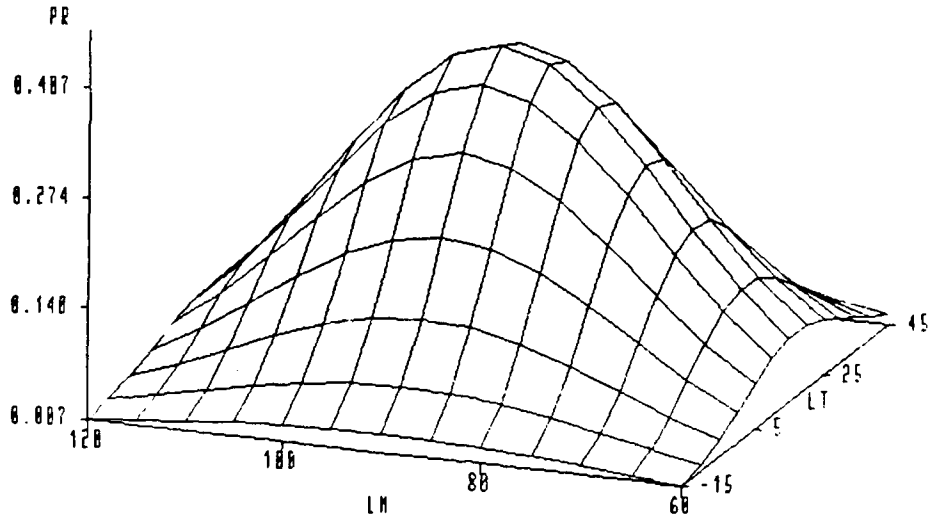
PR
0.407
0.274
0.140
0.007
120
100
80
60
LM
-15
5
25
45
LT

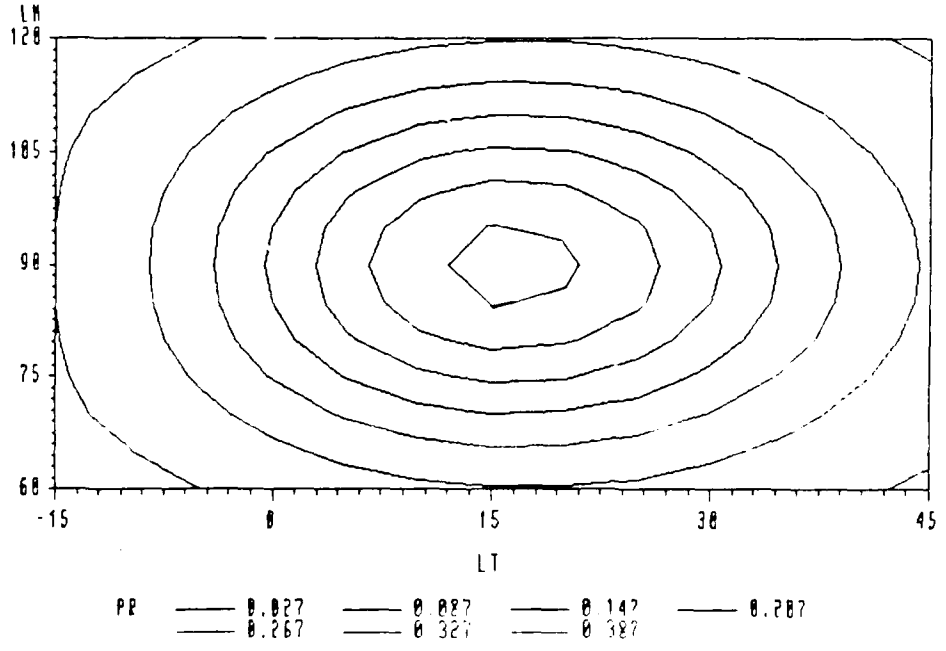
LM
120
105
90
75
60
-15
0
15
30
45
LT
PR
0.027
0.087
0.147
0.207
0.267
0.327
0.387

Case H

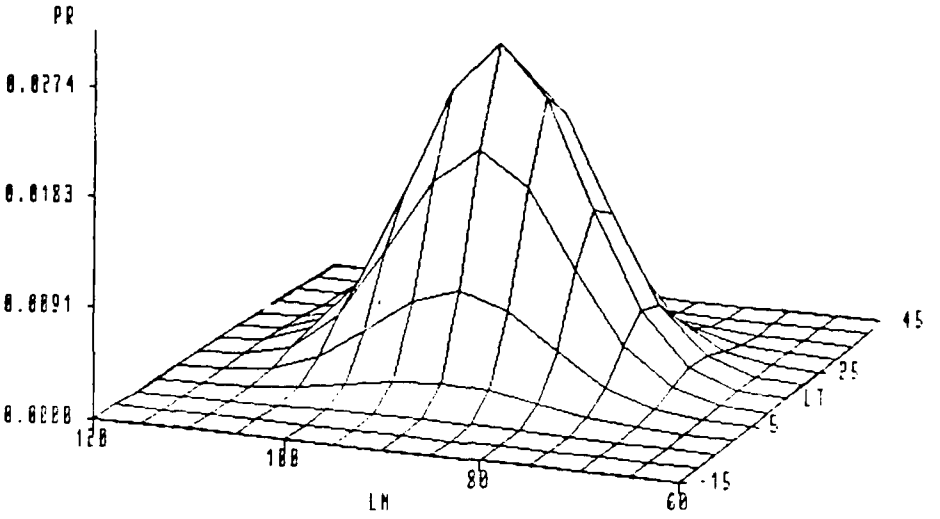
PR
0.0274
0.0183
0.0091
0.0000
120
100
80
60
LM
-15
5
25
45
LT

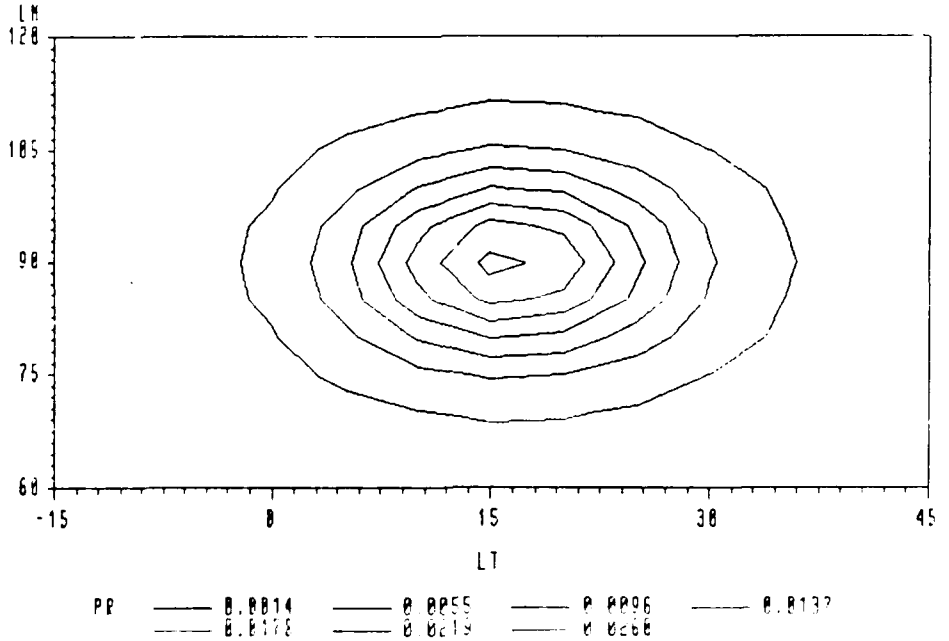
LM
120
105
90
75
60
-15
0
15
30
45
LT
PR
0.0014
0.0055
0.0096
0.0137
0.0178
0.0219
0.0260

Case I

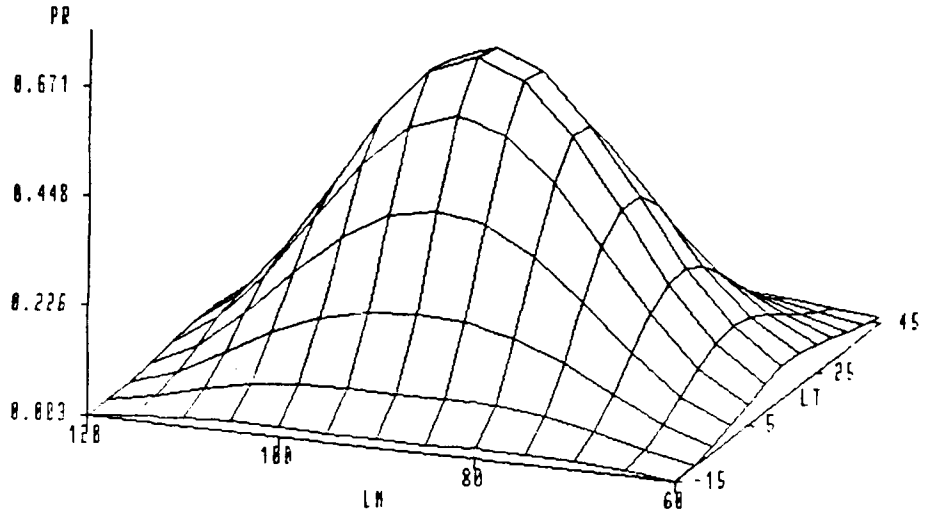
PR
0.671
0.448
0.226
0.003
120
100
80
60
LM
-15
5
25
45
LT

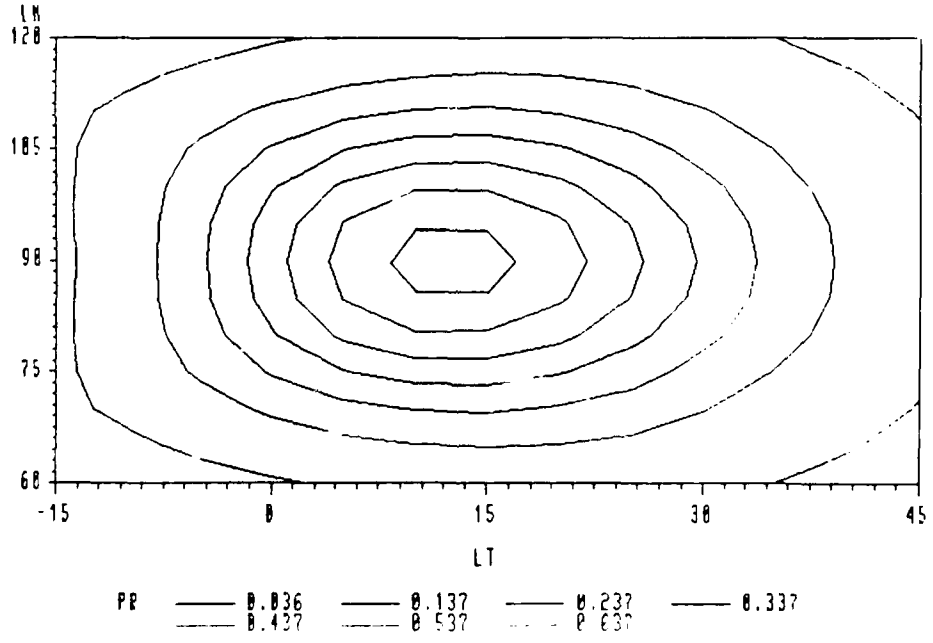
LM
120
105
90
75
60
-15
0
15
30
45
LT
PR
0.036
0.137
0.237
0.337
0.437
0.537
0.637

Case J

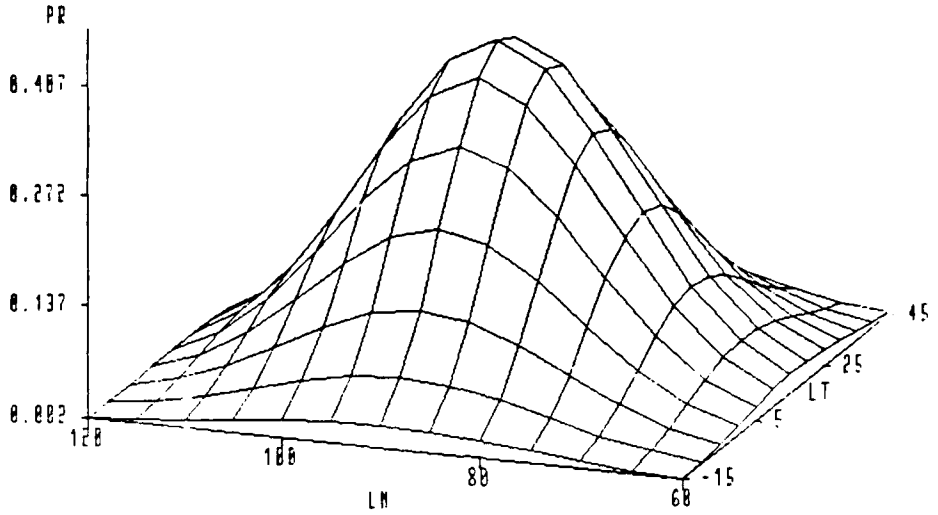
PR
0.487
0.272
0.137
0.002
120
100
80
60
LM
-15
5
25
45
LT

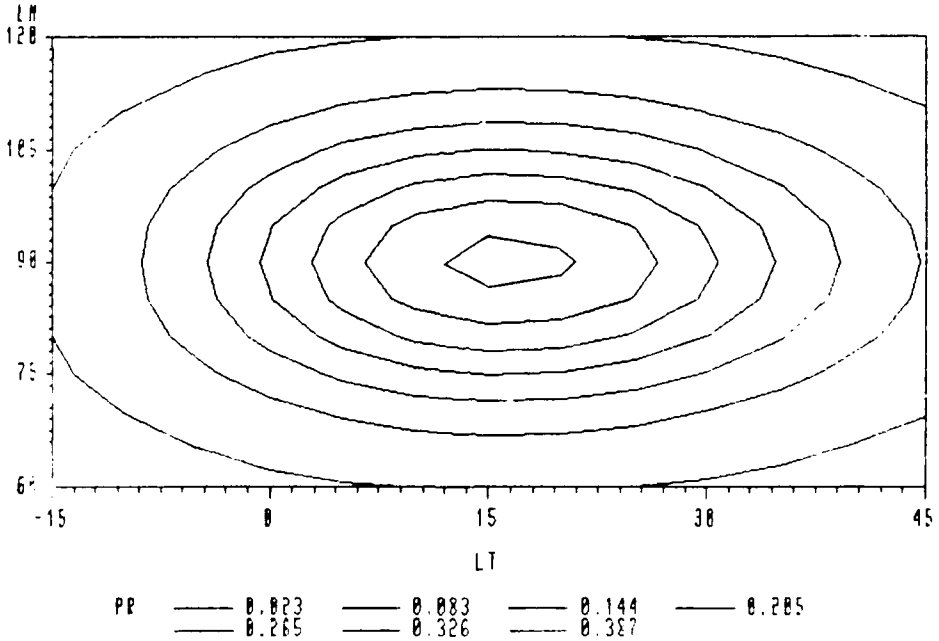
LM
120
105
90
75
60
-15
0
15
30
45
LT
PR
0.023
0.083
0.144
0.205
0.265
0.326
0.387

Bibliography

1. de Neufville, Richard. Applied Systems Analysis: Engineering Planning and Technology Management. New York: McGraw-Hill Publishing Company, 1990.

2. Department of Defense. Confidence Areas for HFDF. Technical Memorandum No. 72-05. May 1972.

3. Drake, Capt David A. and Alfred B. Marsh. "High Frequency Direction Finding Problem Statement." Distributed to students and faculty in the Department of Operational Sciences. Air Force Institute of Technology (AU), Wright-Patterson AFB, OH, Spring 1989.

4. Felix, Lt Robin. High Frequency Direction Finding: Errors, Algorithms, and Outboard. MS thesis, Naval Postgraduate School, Monterey, CA, October 1982 (AD-B071287).

5. Fuller, Gordon. Analytic Geometry (Fifth Edition). Reading, MA: Addison-Wesley Publishing Company, Inc., 1979.

6. Harter, Leon H. "Circular Error Probabilities," American Statistical Association Journal, 55:723-731 (December 1960).

7. Heaps, Melvin G. Accounting for Ionospheric Variability and Irregularity in High Frequency Direction Finding. US Army Atmospheric Sciences Laboratory, White Sands Missile Range, NM, 1981 (AD-A115049).

8. Heaps, Melvin G. et al. High Frequency Position Location: An Assessment of Limitations and Potential Improvements. US Army Atmospheric Sciences Laboratory, White Sands Missile Range, NM, May 1981 (AD-A101217).

9. Hyde, Capt Robin R. Performance Analysis of Combat DF Shipboard Direction Finding System, 16-Channel Receiver. MS thesis, Naval Postgraduate School, Monterey, CA, June 1989 (AD-B140668).

10. Jannusch, Lt Commander Craig M. Statistical Analysis of Three High Frequency Direction Finding Algorithms with Bearing Selection Based on Ionospheric Models. MS thesis, Naval Postgraduate School, Monterey, CA, September 1981 (AD-B061906).

11. Johnson, Capt Krista E. Frequency Assignments for HFDF Receivers in a Search and Rescue Network. MS thesis, AFIT/GOR/ENS/90M-9. School of Engineering, Air Force Institute of Technology (AU), Wright-Patterson AFB, OH, March 1990.

12. Marsh, Alfred B. Unclassified High Frequency Direction Finding (HFDF) Problem Data. Submitted under DOD cover letter, 14 November 1989.

13. Press, S. James. Bayesian Statistics: Principles, Models, and Applications. New York: John Wiley & Sons, 1989.

14. Reilly, M.H. and J. Coran. Confidence Region for the Evaluation of HFDF Single-Site Location Systems. Report No. NRL-MR-5164. Washington: Naval Research Lab, Sep 83 (AD-A133208).